AD-A170 202 NEUROCOGNITIVE PATTERN ANALYSIS OF AUDITORY AND VISUAL 1/1
INFORMATION(U) EEG SYSTEMS LAB SAN FRANCISCO CA
A S GEVINS 15 FEB 86 AFOSR-TR-86-0495 F49620-84-K-0008
UNCLASSIFIED F/G 5/10 NL

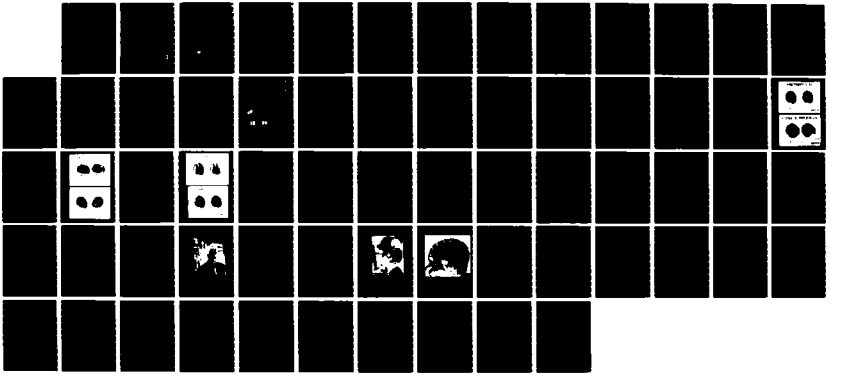

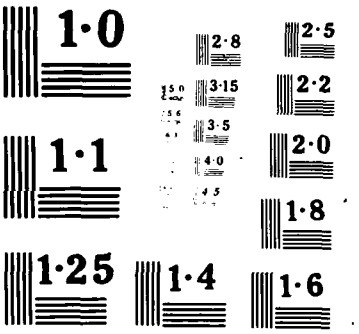
1·0
2·8
2·5
3·15
2·2
3·5
1·1
2·0
4·0
4·5
1·8
1·25
1·4
1·6

(2)

AD-A170 202

REPORT DOCUMENTATION PAGE

1a. REPORT SECURITY CLASSIFICATION: UNCLASSIFIED	1b. RESTRICTIVE MARKINGS:
2a. SECURITY CLASSIFICATION AUTHORITY:	3. DISTRIBUTION/AVAILABILITY OF REPORT: APPROVED FOR PUBLIC RELEASE, DISTRIBUTION UNLIMITED
2b. DECLASSIFICATION/DOWNGRADING SCHEDULE:	
4. PERFORMING ORGANIZATION REPORT NUMBER(S): AFOSR03	5. MONITORING ORGANIZATION REPORT NUMBER(S): AFOSR-TR- 86-0495
6a. NAME OF PERFORMING ORGANIZATION: EEG SYSTEMS LABORATORY; 6b. OFFICE SYMBOL (If applicable):	7a. NAME OF MONITORING ORGANIZATION: DIRECTORATE OF LIFE SCIENCES, AFOSR
6c. ADDRESS (City, State and ZIP Code): 1855 FOLSOM STREET, SAN FRANCISCO, CA 94103	7b. ADDRESS (City, State and ZIP Code): BLDG 410, BOLLING AFB, D.C. 20332
8a. NAME OF FUNDING/SPONSORING ORGANIZATION: AIR FORCE OFFICE OF SCIENTIFIC RESEARCH; 8b. OFFICE SYMBOL (If applicable):	9. PROCUREMENT INSTRUMENT IDENTIFICATION NUMBER: F49620-84-K-0008
8c. ADDRESS (City, State and ZIP Code): BLDG 410, BOLLING AFB, D.C. 20332	10. SOURCE OF FUNDING NOS.

PROGRAM ELEMENT NO.	PROJECT NO.	TASK NO.	WORK UNIT NO.
61102F	2313	A4	

11. TITLE (Include Security Classification): NEUROCOGNITIVE PATTERN ANALYSIS OF AUDITORY AND VISUAL INFORMATION

12. PERSONAL AUTHOR(S): GEVINS, ALAN S.

13a. TYPE OF REPORT	13b. TIME COVERED	14. DATE OF REPORT (Yr., Mo., Day)	15. PAGE COUNT
INTERIM	FROM 84MAR24 TO 86JAN31	86FEB15	60

16. SUPPLEMENTARY NOTATION:

17. COSATI CODES		
FIELD	GROUP	SUB. GR.
0508		
0509		

18. SUBJECT TERMS (Continue on reverse if necessary and identify by block number): PLEASE SEE ATTACHED SHEET ENTITLED "SUPPLEMENT TO FORM DD1473," SECTION 18: SUBJECT TERMS (1 page)

19. ABSTRACT (Continue on reverse if necessary and identify by block number):

PLEASE SEE ATTACHED SHEET ENTITLED "SUMMARY" (page 1)

Original contains color plates: All DTIC reproductions will be in black and white

20. DISTRIBUTION/AVAILABILITY OF ABSTRACT	21. ABSTRACT SECURITY CLASSIFICATION
UNCLASSIFIED/UNLIMITED ☒ SAME AS RPT. ☐ DTIC USERS ☐	UNCLASSIFIED

22a. NAME OF RESPONSIBLE INDIVIDUAL	22b. TELEPHONE NUMBER (Include Area Code)	22c. OFFICE SYMBOL
DR. A. R. FREGLY	(202) 767-5021	AFOSR/NL

DD FORM 1473, 83 APR — EDITION OF 1 JAN 73 IS OBSOLETE. UNCLASSIFIED

SECURITY CLASSIFICATION OF THIS PAGE

AFOSR-TR- 86-0495

NEUROCOGNITIVE PATTERN ANALYSIS OF AUDITORY AND VISUAL INFORMATION

INTERIM REPORT

AFOSR CONTRACT F49620-84-K-008

84MAR24 TO 86JAN31

PREPARED FOR

Dr. A. R. Fregly
Project Contract Officer
Directorate of Life Sciences, AFOSR
Office of Scientific Research
Bolling AFB, D.C. 20332

APPROVED BY

Alan S. Gevins, Director

EEG SYSTEMS LABORATORY

1855 Folsom Street
San Francisco, California 94103
(415) 621-8343

SUPPLEMENT TO FORM DD1473 SECURITY CLASSIFICATION: UNCLASSIFIED

SECTION 18: SUBJECT TERMS

functional neuroanatomy
higher brain functions
EEG
brain models
human performance
operational fatigue
short-term memory
visual stimulus
time-varying processes
statistical pattern recognition
current source density
event-related covariance
P300
functional interdependency
cognition
evoked potentials
parallel processing
performance prediction
preparatory set
performance feedback
digital signal processing
Wigner distribution
spatial deconvolution
source localization
topography
artifact rejection

TABLE OF CONTENTS

LIST OF FIGURES

LIST OF TABLES

EEG SYSTEMS LABORATORY

SUMMARY

The EEG Systems Laboratory has been actively improving the measurement of neuroelectric substrates of human higher brain functions. ~~Our~~ The short-term objective has been to use the EEG to predict decrements in performance consequent to attentional lapses or fatigue. ~~Our~~ The long-term objective is to develop new technologies for enhancing cognitive abilities.

Our laboratory continues to test subjects in highly controlled paradigms. The paradigms test elementary cognitive and perceptuomotor functions critical for flying high performance aircraft and for performing other tasks with a high cognitive load. During FY85, recordings with up to 64 scalp channels have become routine, as has the extended sequence of signal processing operations which extracts minute neurocognitive signals from gigabyte sets of single trial data. Algorithms which register the EEG with magnetic resonance images can now relate the scalp electrode positions to underlying cortical structures. Spectral algorithms for filtering eye-movement contaminants have also been successfully developed. Gateway programs are being implemented to transport multichannel magnetoencephalographic data from several laboratories into our system for analysis.

Data are being analyzed from an interdisciplinary, inter-laboratory study of operational fatigue. This unique set of data consists of 57 channels of neurophysiological, physiological and behavioral data recorded from 4 Air Force fighter test pilots performing several cognitive and perceptuomotor tasks specially designed to require a high commitment of attention, memory, judgement and motor coordination. Recordings were made in 3 sessions dealing with task learning, operational fatigue (about 16 hours of continuous performance), and automatization of task performance.

Initial results on three pilots suggest a differential organization of preparatory prefrontal, premotor and parieto-occipital neuroelectric processes depending upon the load on working memory. In the two pilots examined to date, the ability to maintain this preparatory "set" appears to degrade during fatigue.

Robust measurements of the degree of "functional interdependency" between electrodes have been developed and applied to a bimanual visuomotor judgment task recorded from 7 right-handed men. The results are clear-cut and are consistent with neuropsychological models of the rapidly shifting cortical network which accompanies expectancy, stimulus registration and feature extraction, response preparation and execution, as well as "updating" to feedback about response accuracy. Predictive cue-registered covariance patterns have been identified. These patterns distinguish trials which subsequently had accurate or inaccurate performance.

Along with pilot analyses of intracerebral recordings conducted in collaboration with other laboratories in a primate model, the above results suggest that it is possible to characterize "functional interdependencies" of event-related processing between local neural areas by measuring the wave congruence and lag time of appropriately preprocessed low-frequency macropotentials. Unique determination of the distributed processing network responsible for the observed interdependency patterns is a formidable problem. This is the focus of our ongoing efforts.

EEG SYSTEMS LABORATORY

I. OVERVIEW

A. Senior Scientific Personnel of the EEG Systems Laboratory

Steven L. Bressler, Neurophysiologist
Brian A. Cutillo, Cognitive Scientist
Joseph C. Doyle, Biophysicist
Alan S. Gevins, Director
Douglas S. Greer, Computer Scientist
Judy Illes, Neuropsychologist
Nelson H. Morgan, Electrical Engineer
Ronald K. Stone, Neurologist and Psychiatrist
Roseann White, Operations Manager
Gerald M. Zeitlin, Computer Systems Engineer

B. Publications FY85

1. Gevins, A.S. (1984) Analysis of the electromagnetic signals of the human brain: milestones, obstacles and goals. IEEE Trans. Biomed. Engr., BME-31(12), 833-850.

2. Gevins, A.S., Doyle, J.C., Cutillo, B.A., Schaffer, R.E., Tannehill, R.S., Bressler, S.L. & Zeitlin, J. (1985) Neurocognitive pattern analysis of a visuomotor task: Low-frequency evoked correlations. Psychophysiology, 22, 32-43.

3. Gevins, A.S. (In press) Correlation analysis. In A. Gevins & A. Remond (Eds.), Methods of Analysis of Brain Electrical and Magnetic Signals: Handbook of Electroencephalography and Clinical Neurophysiology (Vol. 1). Amsterdam, Elsevier.

4. Gevins, A.S. (In press) Statistical pattern recognition. In A. Gevins & A. Remond (Eds.), Methods of Analysis of Brain Electrical and Magnetic Signals: Handbook of Electroencephalography and Clinical Neurophysiology (Vol. 1). Amsterdam, Elsevier.

5. Cutillo, B.C. & Gevins, A.S. (In press) Cognitive Brain Signals. In F. Lopes da Silva & A. Remond (Eds.), Applications of Computer Analysis of EEG: Handbook of Electroencephalography and Clinical Neurophysiology (Vol. 2). Amsterdam, Elsevier.

6. Morgan, N.H. & Gevins, A.S. (1986) Wigner distributions of human event-related brain signals. IEEE Trans. Biomed. Engr., BME-33(1), 66-70.

7. Gevins, A.S., Morgan, N.H., Bressler, S.L., Doyle, J.C. & Cutillo, B.A. (In press) Improved event-related potential estimation using statistical pattern classification. EEG Clin. Neurophysiol.

II. OBJECTIVES & SIGNIFICANCE

A. General

We have continued our development of new methods for analyzing the electrical activity of the human brain during higher cognitive functions. Direct measurement of the mass neural substrate of these functions is one prerequisite to developing effective means of enhancing them. Our aim is to refine methods and experimental design which will provide significant steps toward better understanding of the distributed network of mass neural processes associated with human goal-directed behaviors.

Our short-term objective is to predict decrements in performance consequent to attentional lapses or fatigue. Our long-term aim is to lay the foundation for an instrument to measure human neurocognitive processes. There is a pressing need for an instrument which can noninvasively image the functional neuroanatomy of the human brain with high temporal resolution. We foresee great potential applications of this device, including advanced neuropsychological studies of complex cognitive processes, assessment and enhancement of cognitive skills, and clinical studies such as monitoring recovery of function following head injury. We believe that advances in recording EEG and MEG signals, coupled with application of digital signal processing techniques, now make feasible the basic research which will lead to development of an "electromagnetic brain scanner."

B. Specific

Recordings with up to 64 scalp EEG channels during highly controlled tasks are now routine in our laboratory, as is the sequence of signal processing operations required to extract neurocognitive information from sets of single-trial data. More robust measures of the "functional interdependency" (crosscovariance and delay time) between electrodes have been developed and applied to data from a bimanual visuomotor task recorded several years ago. The results are clear-cut and are consistent with neuropsychological models of the cortical activity accompanying expectancy, stimulus registration and feature extraction, movement preparation and execution, and feedback (see Section IV). Many of these results, along with pilot analyses of intracerebral recordings using a primate model, cannot be explained by single equivalent-current dipole source models, but could be understood in the context of multiple, simultaneously active neuronal sources. However, determination of the multiple sources of neural activity associated with cognitive processes remains a formidable problem, since their signals overlap both in time and in space, and are usually smaller than "background" brain activity.

Since the main, unresolved issue is the origin of interdependency patterns measured at the scalp, we are now concentrating on improving our ability to relate scalp recordings to source generator configurations. With improved technologies currently available, we believe that several simultaneous sources can be resolved.

III. NEUROCOGNITIVE PATTERN (NCP) ANALYSIS

A. Overview

The generic term "NCP Analysis" refers to a multi-stepped procedure developed to extract task-related spatiotemporal patterns from the unrelated "noise" of the brain. There have been three prior generations of NCP Analysis. The first (circa 1977) measured background EEG spectral intensities while people performed complex tasks, such as reading and writing. The second (circa 1980) measured single-trial, zero-lag crosscorrelations between 91 pairwise combinations of 15 electrodes recorded during performance of split-second perceptuomotor tasks. The third (circa 1984) measured event-related lagged crosscovariances between all pairwise combinations of up to 26 electrodes on enhanced averages obtained from a controlled sequence of stimuli in which a person prepared for and executed perceptual judgement and motor control tasks and received performance feedback (Gevins et al., 1984a,b; see below). This generation is also being applied to intracerebral recordings from primates. A fourth generation is currently under development. In this generation, because of the large size of the single-trial data sets (up to 150 megabytes for each person), two passes through the data are required to complete the analysis. The first pass selects channels, intervals and trials with task-related information to reduce the amount of data prior to measuring "functional interdependencies" (similarity and time-alignment of waveshapes) between channels. The second pass measures interdependencies between channels on averages obtained from the reduced data set. NCP Analysis is implemented in the ADIEEG-IV analysis system (Fig. 1; see Gevins, In press,a, for discussion of crosscorrelation analysis, and Gevins, In press,b, for discussion of statistical pattern recognition).

B. Current Procedures (Fig. 2)

1. Record up to 64 channels of data and apply the Laplacian operator to the potential measurements to obtain the reference-independent second difference of potential at each non-peripheral scalp electrode location.

2. Create a single, artifact-free data set which will be compared with a reference "baseline" data set. Alternatively, create two data sets that differ according to a specified criterion, such as the hand used for response, but which are otherwise balanced for stimulus, response and performance-related factors. In either case, the two data sets represent conditions which are to be compared.

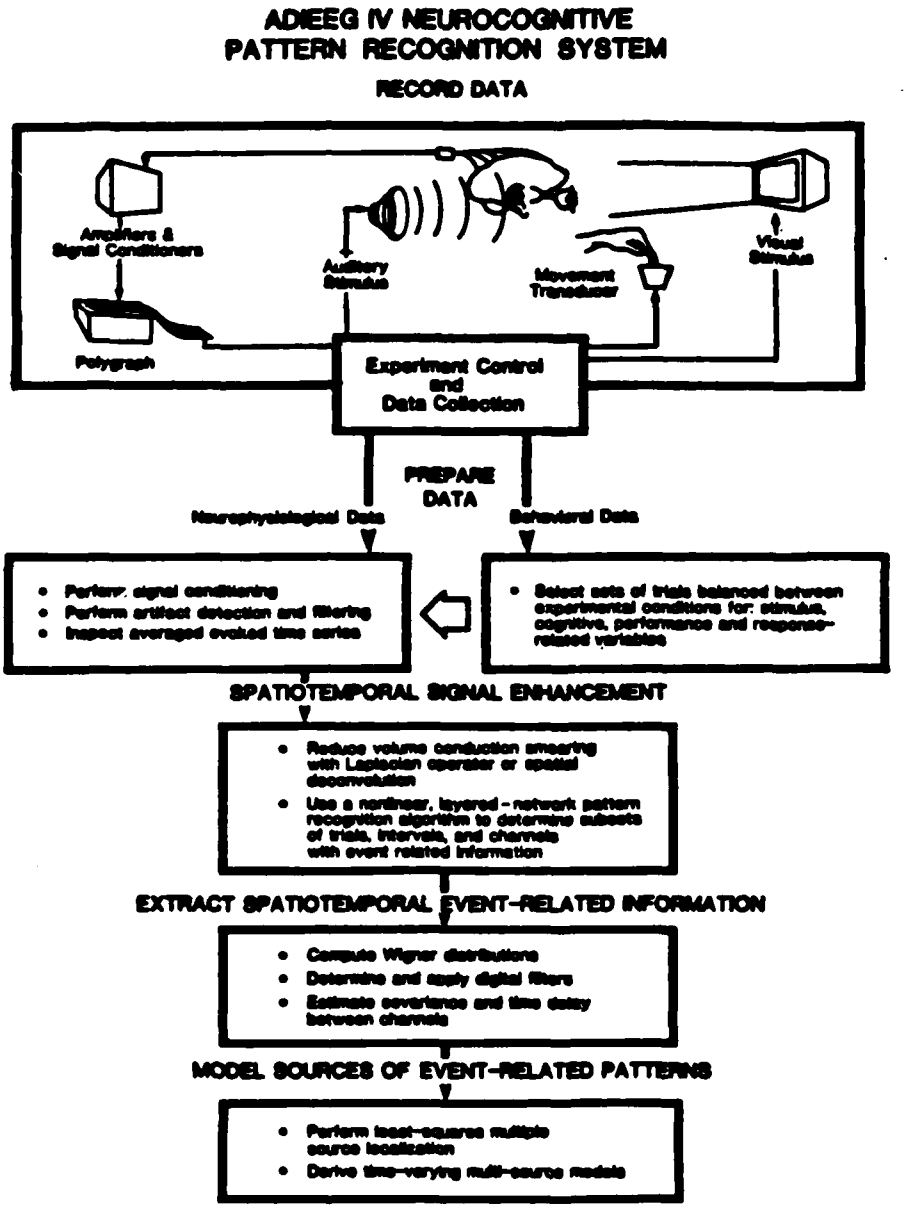

Fig. 1. ADIEEG-IV System for quantification of event-related brain signals. Separate subsystems perform on-line exprimental control and data collection, data selection and evaluation, signal processing and pattern recognition. Current capacity is 64 channels. Digital data tapes from other laboratories are converted into the ADIEEG data format using gateway programs; they are then processed using the same program modules as data collected in the EEG Systems Laboratory. The system is currently implemented on a PDP11 and two Masscomp computers which are connected by high-speed buses. The RSX and UNIX operating systems are used.

NEUROCOGNITIVE PATTERN ANALYSIS

1. SELECT TRIALS WITH EVENT-RELATED SIGNALS
2. COMPUTE ENHANCED AVERAGE ERPS AND FILTER
3. DEFINE WINDOWS FOR COVARIANCES FROM ERP PEAKS
4. COMPUTE COVARIANCES AND DELAYS BETWEEN PAIRS OF CHANNELS
5. GRAPH MOST SIGNIFICANT COVARIANCES IN EACH WINDOW

Fig. 2(a). NCP Analysis.

Fig. 2(b). Illustration of the covariance diagram, indicating electrode positions and showing the relationship of a covariance line to the theta- filtered averaged event-related timeseries from the 2 corresponding elec- trodes. In all covariance diagrams, the width of a line indicates the magnitude of covariance between 2 electrodes and its color indicates the magnitude of time delay. When the color of the arrow is the same as the covariance line, the covariance is positive; when the arrow is gray, the covariance is negative. The arrow points from leading to lagging channel. (Specific values are given on each diagram.)

F3

FZ

F4

AC3

ACZ

AC4

C3

CZ

C4

APZ

P3

PZ

P4

AOZ

Covariance

p < .05

$p < 10^{-3}$

$p < 10^{-5}$

Delay

(milliseconds)

0 - 15

16 - 31

32 - 47

48 - 79

80 +

Arrow points away from channel that is leading.

Arrow color indicates sign of covariance.

Positive

Negative

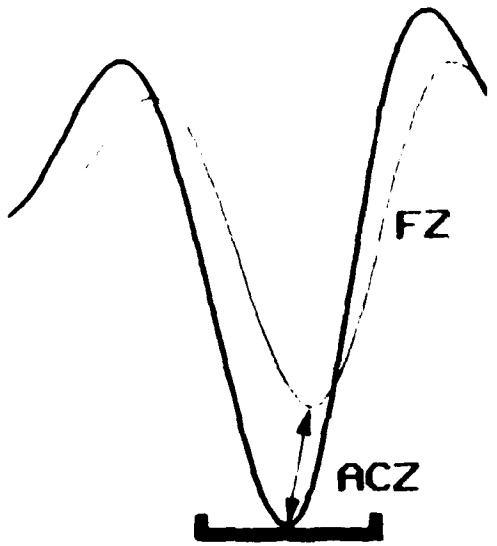

EEG SYSTEMS LAB

Signal enhancement:

3. Compute average event-related timeseries for stimulus, response, cue or feedback for each person, and use the latencies of peaks to determine centerpoints of analysis windows for pattern recognition analysis on the sets of single trials. Adjust the window size to span the peak (usually 125 to 250 msec). (Set other windows at stimulus and response times.)

4. Apply a 7 Hz low-pass filter to the timeseries and then decimate appropriately. Use 3-7 timeseries values as features.

5. Partition the event-related and "baseline" data (or the data of the two conditions) into training and validation sets. For each channel, apply a layered-network pattern recognition algorithm (a type of discriminant analysis---see Gevins 1980, 1984, In press,b) to generate equations which represent invariant differences between event-related and "baseline" data sets or between two conditions in the analysis interval.

6. Test the equations with the validation data to determine which electrodes differ significantly between conditions. Set the level of significant classification well above that attained with the data randomly assigned to two pseudo-conditions, as determined by separate analysis.

7. Draw diagrams showing which electrodes contain task-related information in each interval.

8. Collect trials with task-related signals (i.e., trials correctly classified in the validation set), and compute "enhanced" averages using those trials which were correctly classified in a majority of the significant channels. Graph isopotential contours at selected time points.

Between-channel interdependency analysis:

9. Filter enhanced averages using Gaussian FIR filters in frequency bands determined from a Wigner distribution of the enhanced averages. Compute multi-lag crosscovariance functions between all channel pairs in each analysis window. Window centerpoints are determined from peak latencies and window widths are derived from the dominant frequency of each band.

10. Compute a delay estimate for each pair from the lag with maximum absolute covariance. Compute the significance of this covariance by comparison to a reference noise distribution derived from the averages themselves (see below). Display most significant channel-pairs and their time delays.

The above method of computing covariances from enhanced averages was used to generate the new results in Section IV. A related method using unfiltered correlations between intracerebral electrodes was applied to primate data.

C. Previous Experimental Findings

1. Complex perceptuomotor and cognitive activities such as reading and writing produce unique, spatially differentiated scalp EEG spectral patterns. These patterns had sufficient specificity to identify the type of task (Gevins et al., 1979a). These results agree with previous reports of hemispheric lateralization of "spatial" and "linguistic" processing.

2. When tasks are controlled for stimulus, response and performance-related factors, complex cognitive activities such as arithmetic, letter substitution and mental rotation have identical, spatially diffuse EEG spectral scalp distributions. Compared with staring at a dot, such tasks have approximately 10% reductions in alpha- and beta-band spectral intensities (Gevins et al., 1979b,c). This reduction may be an index of task workload. Since no patterns of hemispheric lateralization were found, this study suggests that previous and most current reports of EEG hemispheric lateralization may have confounded electrical activity related to limb and eye movements and arousal with those of mental activity per se (Gevins et al., 1980).

3. Split-second visuomotor tasks, controlled so that only the type of judgment varied, are associated with complex, rapidly shifting patterns of inter-electrode correlation of single-trial brain potential timeseries. Differences between spatial and numeric judgments are evident in the task-cued prestimulus interval. Complex and often lateralized patterns of task-related correlation changed with split-second rapidity from stimulus onset to just prior to response, at which time there was no difference between tasks (Gevins et al., 1981). This suggests that once task-specific perceptual and cognitive processing is completed, a motor program common to both tasks is being executed.

4. Rapidly shifting focal scalp patterns of differences between tasks can be extracted with NCP Analysis. The move and no-move variants of a split-second visuospatial judgment task, which differed in expectation, in type of judgment, and in response (move or no-move), were associated with distinctly different patterns of single-trial evoked correlation between channels (Gevins et al., 1983, 1985). These results are consistent with neuropsychological models of analogous tasks derived from functional deficits of patients with focal lesions. Further, they suggest that although simple perceptuomotor tasks are associated with a complex dynamic mosaic of brain potential patterns, it is possible to isolate foci of maximal differences between tasks. It is clear that without a split-second temporal resolution it would not be possible to isolate rapidly shifting lateralizations and localizations which are presumably associated with successive stages of task-related processing.

5. The focal patterns of evoked correlation derived by NCP Analysis significantly distinguished the single-trial data of 7 of the 9 people in the above study. This suggests that consistent neurocognitive processes were measured in the majority of right-handed male research participants (Gevins et al., 1985).

6. Analyses of pilot intracerebral primate data (recorded at Rebert's laboratory at SRI) revealed rapidly shifting correlation patterns between hippocampus, substantia nigra, premotor cortex, ventroanterior nucleus of the thalamus, and the midbrain reticular formation which distinguished go and no-go visuomotor tasks. Interdependencies of the hippocampus with other loci were prominent in the "go" condition (which lead to reward) but not in the no-go condition during intervals from 240 to 578 msec after the cue. The patterns were characterized by delays of up to 72 msec or more between loci.

D. Comparison of NCP Analysis, ERP Techniques and Topographic Maps

Our experiments and analyses are grounded on the body of information gained from ERP research and have the same underlying goal: to resolve spatially and temporally overlapping, task-related neural processes (Chapters 3, 5, 10, 12, 13, 14, 16, 17 & 18 in Gevins & Remond, In press). Our approach differs in several ways from the currently popular ERP paradigms which: (a) extract a few features from averaged ERPs by peak picking or principal components analysis (PCA); and (b) perform hypothesis testing on the features with ANOVA. First, because neurocognitive processes are complex, we are concerned with spatiotemporal task-related activity recorded by many (currently up to 64) scalp electrodes in many (currently about 20) time intervals spanning a 5-second period extending from before a cue, through stimulus and response, to presentation of feedback. By contrast, most ERP experiments are concerned with measurement of one to a few "components" associated with a single stimulus or response registration in a few channels in an epoch under one second. Additionally, NCP Analysis quantifies neurocognitive activity in terms of a variety of parameters, including measurement of "functional interdependencies" between channels, rather than just amplitude and latency of ERP components. This increased dimensionality of parameterization may facilitate the measurement of more subtle aspects of neurocognitive processes.

Second, the questionable assumption of a multivariate normal distribution of very brief brain potential timeseries is not made in the first signal enhancement pass of NCP Analysis, while robust statistics are used in the second pass to assess the significance of covariances. Third, feature extraction and hypothesis testing are performed as a single process which determines the differences in signal properties between the conditions of an experiment, or their differences with respect to a "baseline." We think that this is more effective than feature extraction techniques, such as PCA, which are based on possibly irrelevant criteria (such as statistical independence of features regardless of discriminating power). Fourth, in NCP Analysis task-related patterns of consistency can be extracted from sets of single-trial data. Significant results may be obtained as long as there is a pattern of consistent difference, even when the means of the two data sets are not significantly different.

NCP Analysis should also be distinguished from attractive topographic color displays of the individual time points of 16-20 channels of averaged ERPS or EEG spectra, or the difference between such measures

and a set of normative data. NCP Analysis uses extensive signal processing and pattern recognition algorithms on up to 64 channels to extract minute "neurocognitive" signals from the unrelated background "noise" of the brain, computes between-channel interdependency patterns and displays their scalp distribution in topographical diagrams. (See Gevins & Remond, In press, for a thorough treatment of all types of brain electromagnetic signal analyses.)

IV. RECENTLY COMPLETED AND ON-GOING EXPERIMENTS

A. Bimanual Numeric Visuomotor Experiment

The aim of this experiment, the recordings of which were largely funded by the Office of Naval Research (ONR), was to measure the rapidly changing, spatially distributed, neurocognitive patterns associated with execution of precise right- and left-hand finger movements (Diewert & Stelmach, 1978; Newell, 1978; Sternberg et al., 1978; Rosenbaum et al., 1984) during complete 5-second-long task trials, from cued preparation, through post-stimulus perceptual and cognitive processing, and response execution, to the "updating" associated with feedback (Fig. 3).

EEG signals from 26 scalp electrodes referenced to a midline anteroparietal electrode, vertical and horizontal eye movements (EOG), and flexor digitori muscle potentials (EMG) were digitized on magnetic tape at 128 Hz from .75 sec before the cue to one second after feedback. The Laplacian operator was applied to the EEG potentials by computing the curvature of the potential field about each electrode. Two independent raters edited the data for artifacts by visual inspection of EEG, EOG and EMG polygraph channels. Trials with any sign of artifact were eliminated, as were trials with slow, bimodal or delayed responses, and trials with any sign of flexor digitori activity in the cue-to-stimulus epoch. For each event, comparison between conditions (e.g., right-vs-left hand movement), was performed on artifact-free trials, balanced between conditions for relevant behavioral variables (e.g., response onset time, response movement force, velocity, acceleration and duration).

Spatiotemporal neuroelectric patterns were quantified by measuring the covariance (similarity of waveshape and timing) over brief intervals of highly processed averaged event-related timeseries recorded from different locations. Between-channel covariances from filtered averages were examined in two frequency bands, "delta" (0.1-3 Hz) and "theta" (4-7 Hz), during 25 intervals from the cue to after the feedback. Delays, defined as the lag time of maximum covariance, were examined to plus or minus 125 msec. Unless otherwise noted, all covariances described were from "theta-band" filtered averages. Since this was the first complete set of data available for our new analyses, the specific results are briefly described here as illustrative of the methods. Unless otherwise stated, all covariances were from theta-filtered waveforms.

1. Prestimulus Preparatory Set. Neurocognitive patterns related to differential preparation of right- and left-hand responses were measured in the cue-to-stimulus epoch. The 7-person cue-

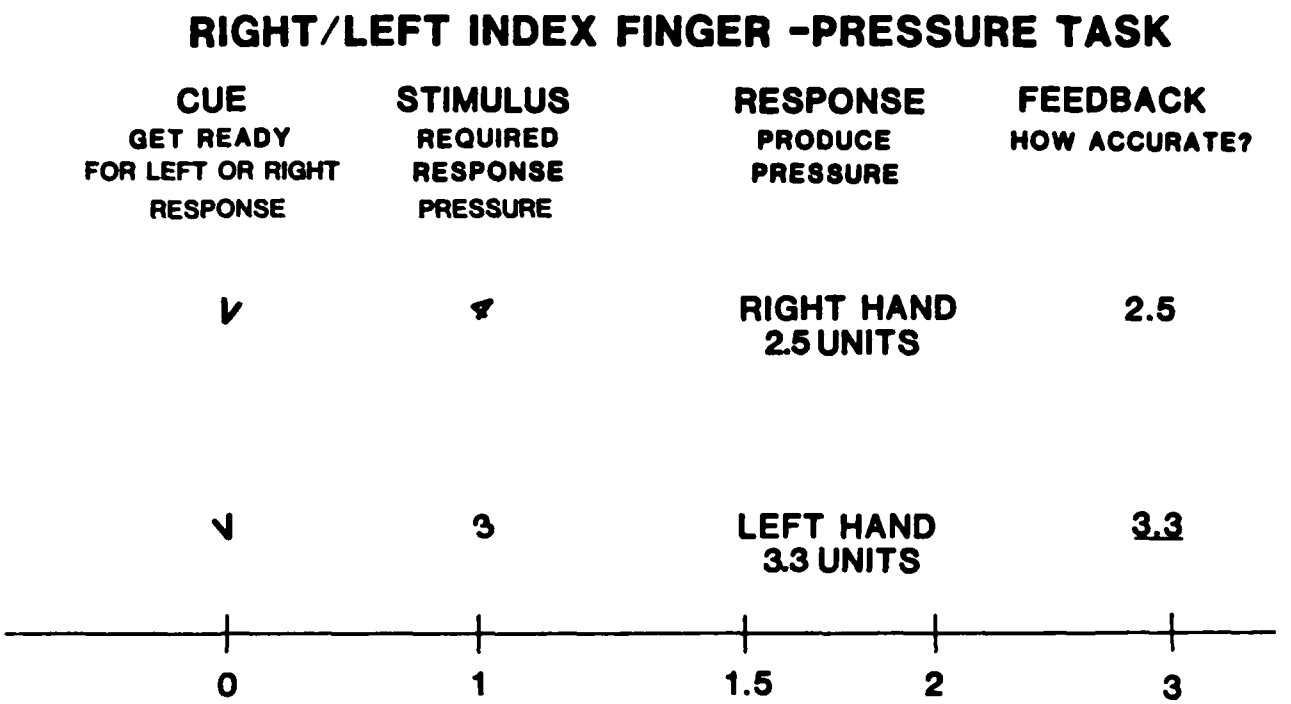

Fig. 3. R/L Task Sequence.

registered Laplacian timeseries contained two distinct waves corresponding to the early and late components of the Contingent Negative Variation (CNV): a broad "O wave" between 250 and 500 msec followed by a slow ramp-like shift leading to the stimulus. Evidence of a pre-stimulus hand-specific set occured in covariance patterns for "delta-band" (0.1-3 Hz) filtered data in the 500 msec preceding the stimulus during the late CNV wave. The most obvious difference between conditions was the predominantly left-sided patterns for right cue, compared to the mixed patterns for left cues. These patterns tended to focus on particular frontal, central and parietal electrodes over areas consistent with cortical loci of preparatory motor sets suggested by clinical neuropsychological studies (Fig. 4). Different patterns were found for trials which had subsequently accurate or inaccurate visuomotor performance (Fig. 9), suggesting that a preparatory set, composed of an attentional and a somesthetic-motor component, is necessary for good performance. To further verify the cerebral origin of the covariance patterns, EOG and EMG channels were submitted to a mathematical pattern classification program. The objective was to determine if these channels could significantly classify right-hand accurate from right inaccurate trials, and left-hand accurate from left inaccurate trials. The eye movement channels were delta filtered, and down sampled to 16 samples/sec over an interval 375 msec wide with a 687 msec center; EMG channels were half-wave rectified. Neither the EOG nor EMG channels significantly classified trials at the level better than chance (50%).

2. Post-stimulus Processing of Move and No-move Trials. Differences between move and no-move trials were examined in post-stimulus intervals spanning early and late event-related waves. Right- and left-cued no-move trials were examined for differences related to miscued hand (violation of preparatory set). Covariance patterns in early intervals were similar for right- and left-hand move trials (Fig. 5), until the interval centered at 312 msec, where they became highly complex. Covariance patterns for right- and left-cued no-move trials differed from move patterns from the first post-stimulus interval, but they were quite similar to each other by the interval centered at 312 msec. During this interval which spanned the large early P300 wave and included a portion of the latter P300 wave, lateral frontal and midline parietal electrodes lead aCz, which in turn lead Fz (Fig. 6).

3. Between-Hand Movement Analysis. Differences between right and left-hand move trials were examined in response-registered data in intervals before and after response onset. The 7-person waveform was largest at aCz and consisted of: (1) a slow ramp-like shift beginning about 450 msec before movement onset (Readiness Potential), (2) an increase in slope at EMG onset (Motor Potential) which peaked 62 msec after response onset, and (3) the Response After-Potential 187 msec after response onset. This anterior midline precentral electrode, overlying the pre-motor supplementary motor cortices, was the focus of all movement-related covariance patterns, and there was a consistent long-delay covariance between the anterior midline, precentral and midline prefrontal electrodes in these patterns (Fig. 7). The pattern for the Motor Potential clearly reflected the sharply focused current sources and sinks spanning the hand areas of motor cortex. Both the Laplacian topography and the covariance patterns suggest distinct source generator configurations for the Readiness Potential, Motor Potential and Response After-Potential.

4. Feedback Analysis. Neurocognitive patterns following "win" and "lose" feedback for move trials were examined for differences in "amount of updating" and hand-specific effects. These results were compared to feedback for no-move trials, where no "motor system updating" was required. Evidence was found in feedback-registered covariance patterns and averaged Laplacian timeseries which may reflect different degrees of updating of motor systems when given information about response accuracy. Feedback trials in which no adjustment of the motor system was required elicited very small P300 peaks. Feedback for accurate responses elicited a larger amplitude "early P300," while feedback for inaccurate responses elicited a larger amplitude in the later P300. The covariance pattern in the interval spanning these waves was far more complex for inaccurate trials, involving foci of leading covariances at parietal sites, of lagging covariances over dorsolateral prefrontal areas, and mixed delays at the anterior precentral site (Fig. 8). It would be difficult to explain these different patterns, which included delays of up to 80 msec between electrodes 3 cm apart, solely in terms of volume-conducted activity from one or two subcortical and/or cortical generators.

B. Fatigue Experiment

1. Overview. Data are currently being analyzed from an interdisciplinary, inter-laboratory study of operational fatigue. This unique set of data consists of 57 channels of neurophysiological, physiological and behavioral data recorded from several Air Force fighter test pilots performing cognitive and perceptuomotor tasks specially designed to require a high commitment of attention, memory, judgement and motor coordination. Recordings were made in four sessions, on three days, dealing with task learning, operational fatigue (about 16 hours of continuous performance), and automatization of task performance.

Initial results on three pilots suggest a differential organization of preparatory prefrontal, premotor and parieto-occipital neuroelectric processes depending upon the load on working memory. In the first two pilots examined so far, the ability to maintain this preparatory "set" appears to degrade during fatigue.

The job performance of a fatigued person may be described as "having no film in the camera." It is a common observation that persons in such a condition may be able to acceptably perform rote behaviors, but are unable to respond to sudden unexpected situations which require full commitment of higher cognitive functions. Furthermore, fatigue can produce momentary lapses of attention, decision processes and perceptuomotor performance. One characteristic of fatigue is a reduced ability to perceive one's diminished capacity. Since there are many situations where momentary inability to respond effectively to an unexpected situation, a lapse of attention, may result in serious or fatal consequences, it is important to know more about the behavioral, physiological and neurophysiological signs which may preceed such states. Such knowledge could lead to new, more effective methods of detecting the precursors of the impaired condition, before any impairment is evident in actual performance.

Fig. 4. Patterns of inter-electrode covariances for Left and Right Cue conditions computed from "delta-band" (.1 to 3 Hz bandpass) filtered data of 7 persons in a 375 msec wide interval centered at 687 msec after the cue. Patterns for right cues are mostly left-sided; patterns for left cues are mostly right-sided. The midline anterior central area is a focus of covariances in both conditions, reflecting activity of premotor and supplementary motor cortex. Left frontal covariances are prominent for both hands.

Fig. 5. Stimulus-evoked covariance patterns for Left and Right Move conditions on a 187 msec wide interval centered at 62 msec after stimulus onset. Covariances were computed from "theta-band" (4 to 7 Hz bandpass) filtered data. At this interval, covariances show a similar pattern: midline posterior parietal electrode covariances lead midline anterior parietal, which lead midline premotor electrode covariances. Note additional covariances from the right posterior parietal electrodes for the right-rotated foveal stimuli. These may reflect the projection to the scalp from generators deep in the left calcarine fissure.

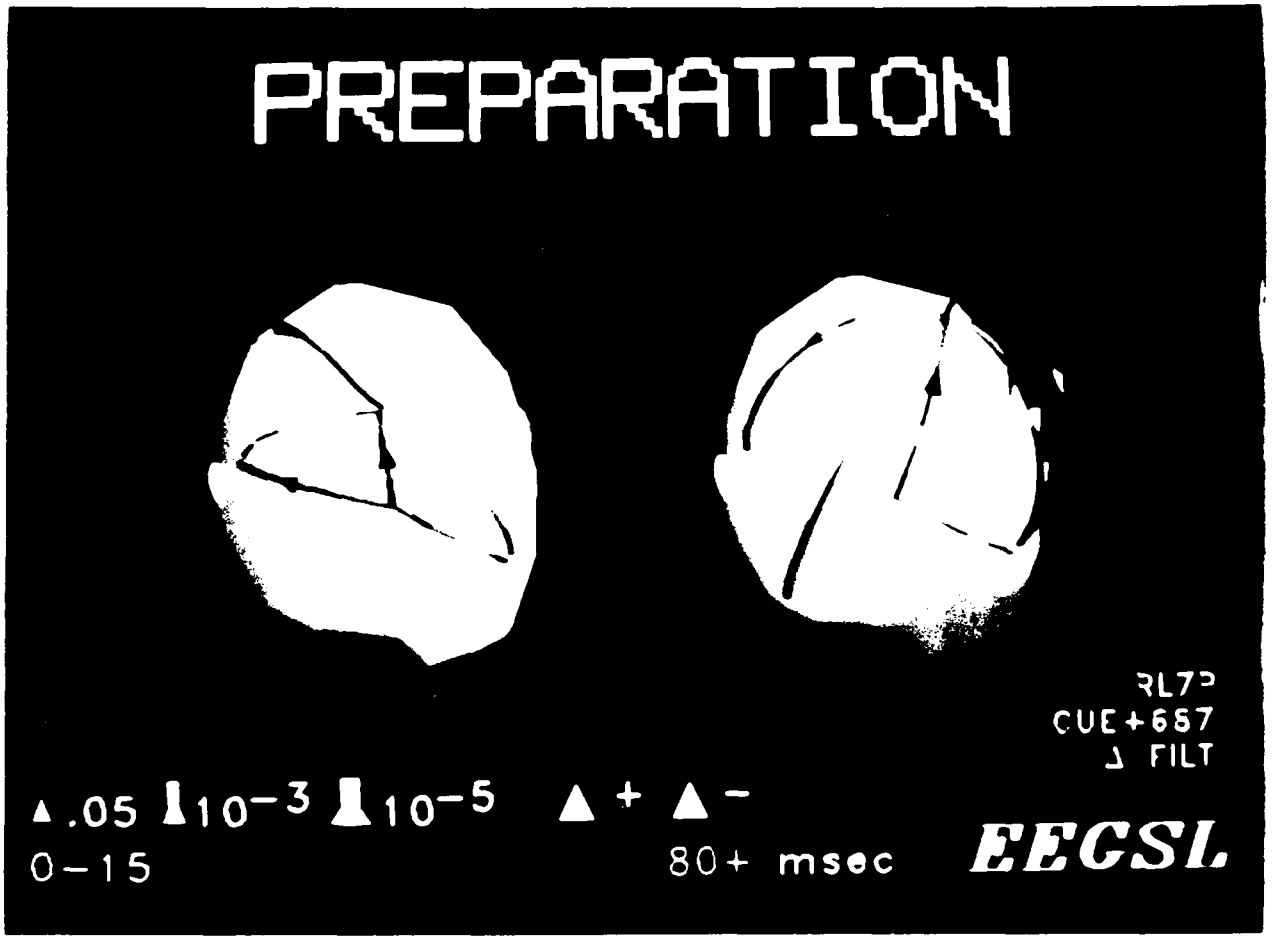
PREPARATION
RL7P
CUE+687
Δ FILT
▲.05 ▮10⁻³ ▮10⁻⁵ ▲+ ▲−
0−15
80+ msec
EEGSL

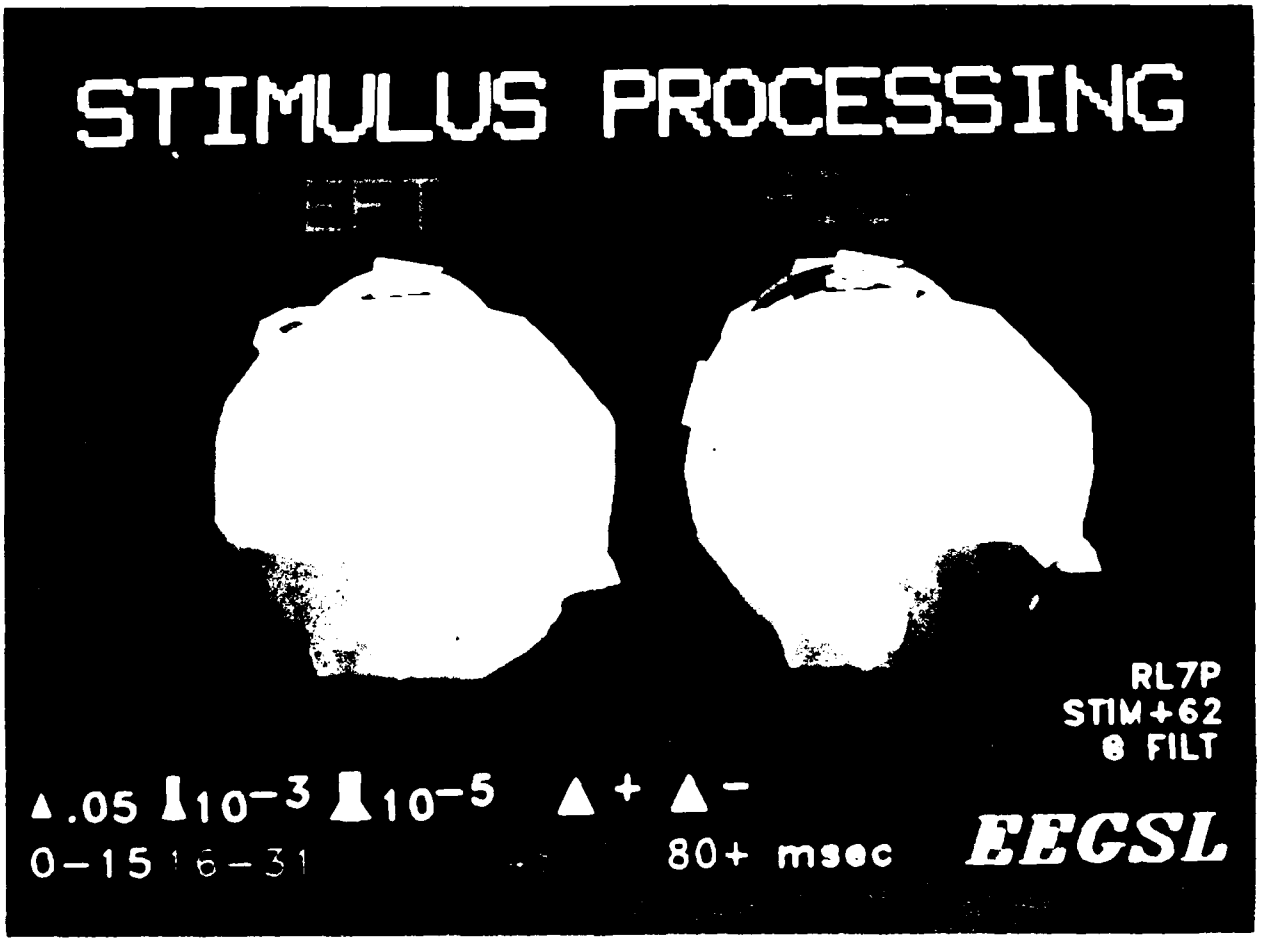
STIMULUS PROCESSING
RL7P
STIM+62
θ FILT
▲.05 ▮10⁻³ ▮10⁻⁵ ▲+ ▲−
0−15 16−31
80+ msec
EEGSL

Fig. 6. Stimulus-evoked covariance patterns for the Left and Right Move and No-Move trials. Covariances were computed from "theta-band" (4 to 7 Hz bandpass) filtered data on a 187 msec wide interval centered at 312 msec after stimulus onset. The midline premotor electrode lags the left and right prefrontal electrodes, as well as the midline prenatal electrode in the No-Move trials. This may be a sign of motor inhibition.

Fig. 7. Covariance patterns for Left and Right Move trials, computed from "theta-band" (4 to 7 Hz bandpass) filtered data, 62 msec after movement onset. At the peak of the finger pressure, covariance patterns are appropriately contralateral to the hand used. The midline premotor electrode, which is the focus of all covariances, leads the prefrontal electrodes by 16-31 msec.

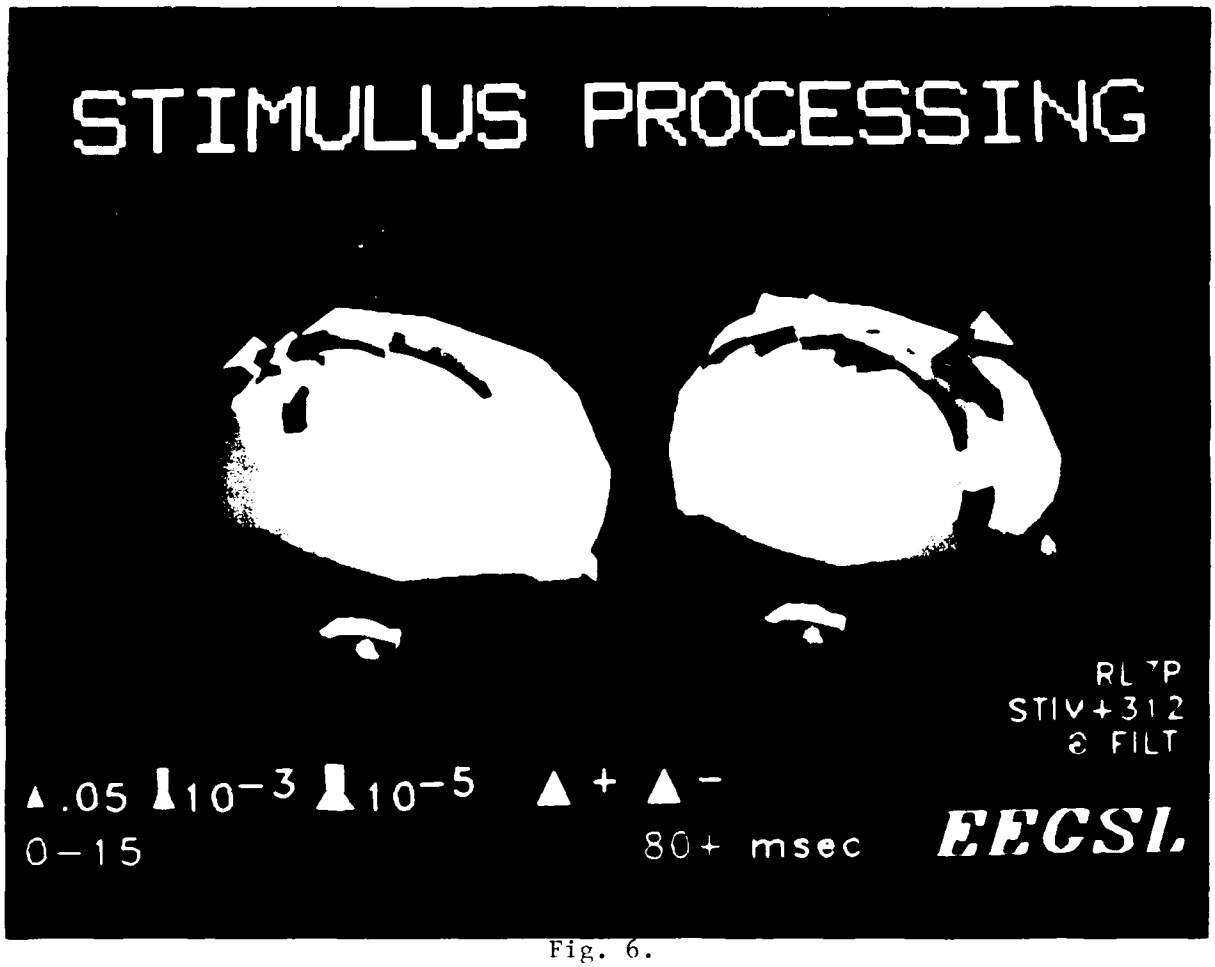
STIMULUS PROCESSING
RL 7P
STIV+312
∈ FILT
▲.05 ▌10⁻³ ▌10⁻⁵ ▲+ ▲−
0−15
80+ msec
EECSI.

Fig. 6.

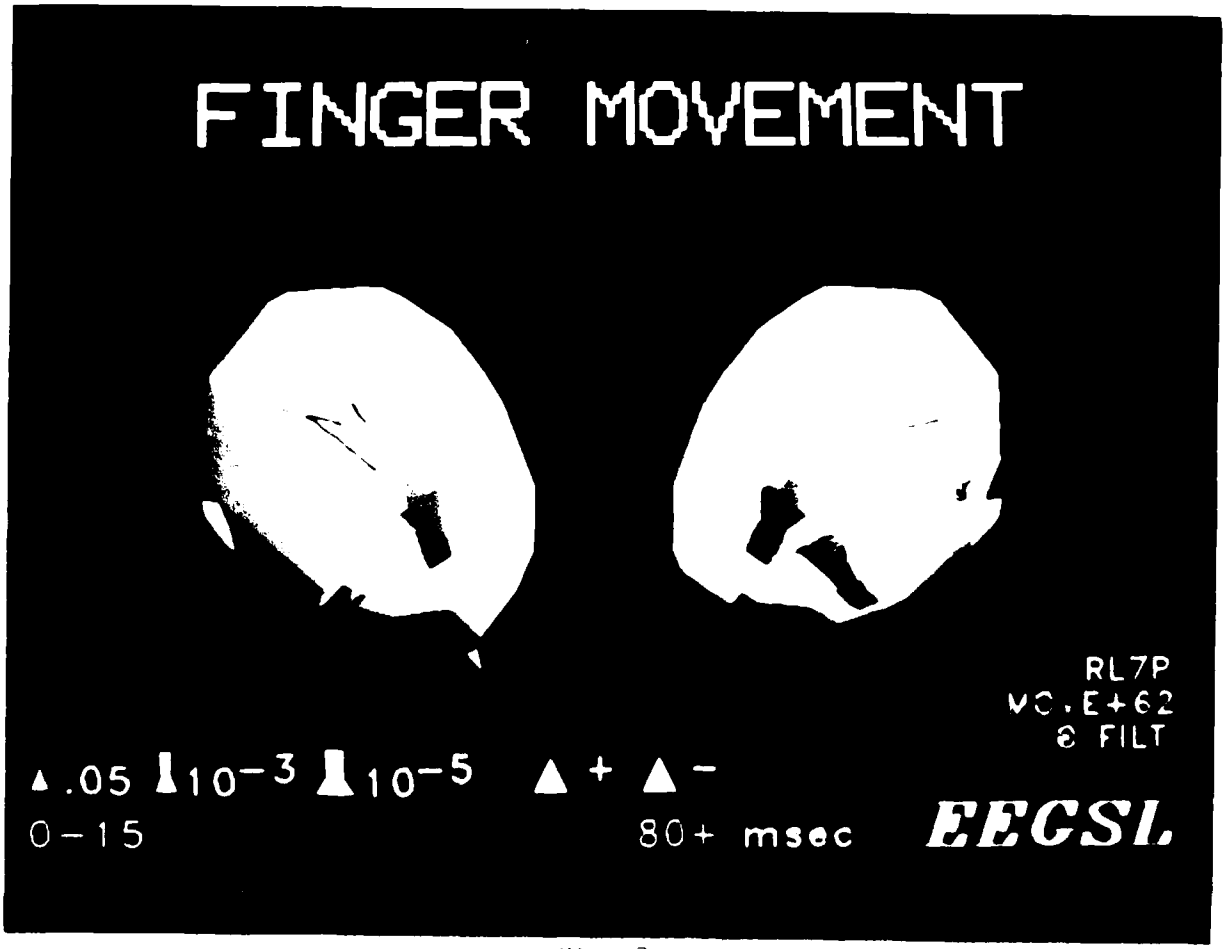
FINGER MOVEMENT
RL7P
VC.E+62
∈ FILT
▲.05 ▌10⁻³ ▌10⁻⁵ ▲+ ▲−
0−15
80+ msec
EECSI.

Fig. 7.

Fig. 8. Covariance patterns for accurate and inaccurate feedback in left-hand trials computed from "theta-band" (4 to 7 Hz bandpass) filtered data in a 187 msec wide interval, centered 375 msec after feedback. There is a common pattern involving covariances from midline occipital and parietal to midline premotor and right prefrontal electrodes. When the responses were inaccurate, the feedback pattern additionally included the left prefrontal electrode. The right frontal and midline premotor components common to both accurate and inaccurate trials may reflect "motor recalibration," while the left prefrontal component in inaccurate trials may reflect "updating" in attentional set for behavioral verification.

Fig. 9. Covariance patterns reflecting prestimulus differences between accurate and inaccurate trials, computed from "delta-band" (.1 to 3 Hz bandpass) filtered data in a 375 msec wide interval centered 687 msec post cue, i.e., 313 msec pre-stimulus. Note the greater complexity of subsequently accurate trials. Covariances overlying left prefrontal cortex are prominent in accurate trials, but are absent in inaccurate trials. This may reflect the involvement of the left prefrontal cortex in establishing a preparatory set necessary for accurate performance.

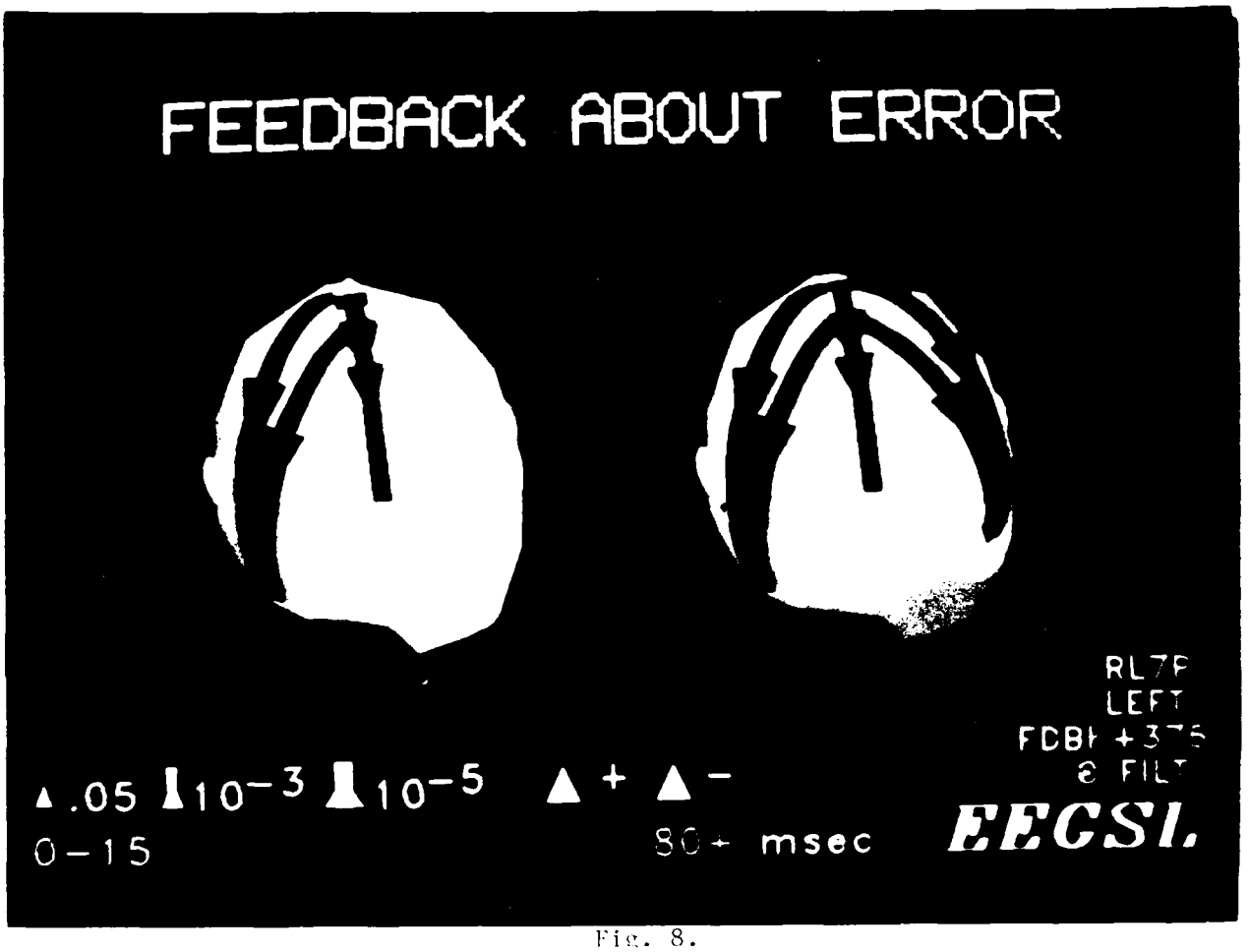
FEEDBACK ABOUT ERROR
RL7P
LEFT
FDBK +375
Δ FILT
▲.05 ▌10⁻³ ▌10⁻⁵ ▲+ ▲−
0−15
80+ msec
EECSL

Fig. 8.

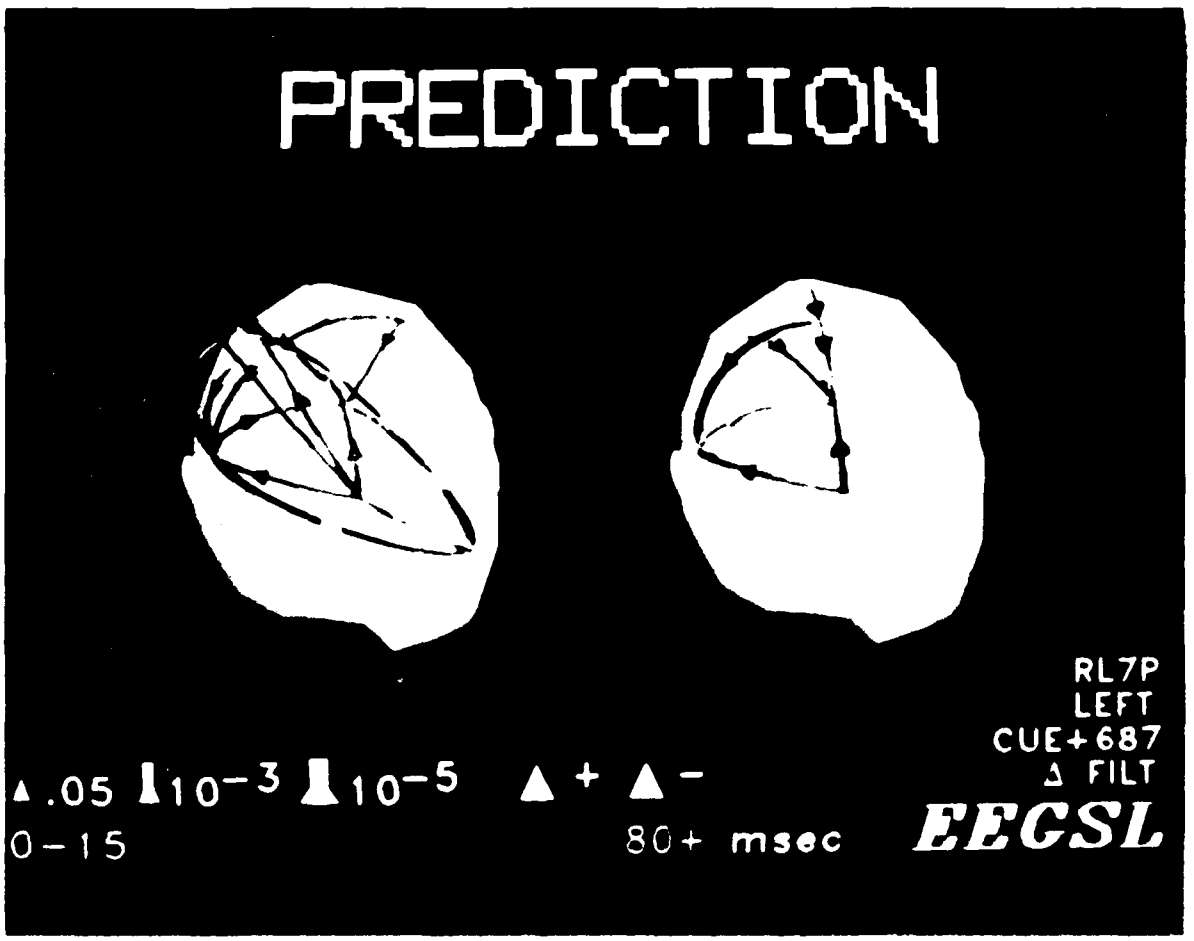
PREDICTION
RL7P
LEFT
CUE+687
Δ FILT
▲.05 ▌10⁻³ ▌10⁻⁵ ▲+ ▲−
0−15
80+ msec
EECSL

Only a very few studies have attempted to measure behavioral, physiological and neurophysiological variables during controlled fatigue-inducing conditions. The study of operational fatigue rests on the ability to produce a state of performance decrement in an experimental situation specifically controlled for the factors of initial task learning and subsequent automatization of performance, so that the effects of fatigue can be distinguished from learning and automatization. The recording session must extend from a state of well-practiced, alert performance to later stages in which decrements of performance due to fatigue are clearly evident in performance measures. Also, a follow-up recording in an unfatigued state must be made in order to determine whether any results observed in the fatigued state were actually due to automatization of task performance over many hundreds of trials. It is crucial that the tasks be sufficiently taxing in the alert state, yet able to be performed in the fatigued state. These tasks should have reasonable construct and face validity for real-life situations, such as piloting an aircraft, and must meet the rigorous requirements of neurophysiological recording and analysis.

2. Experiment Development. Over the last four years, an interdisciplinary team of researchers from four organizations collaborated on designing a study of operational fatigue. The group consisted of James Miller, USAF School of Aerospace Medicine, San Antonio; Henry Jex and James Smith, Systems Technology Inc., Los Angeles; John Stern, Washington University, St. Louis; and Alan Gevins and other personnel of the EEG Systems Laboratory.

After some development, a suitable paradigm was developed which implemented the above criteria. In February 1983, a pilot recording was made at the EEG Systems Laboratory involving a single fatigue session in a previously practiced subject. It consisted of four repetitions of the performance of 2-hour modules ("sorties"), each sortie containing four tasks. Two tasks tested rote visuomotor performance, one with a moderate task load (subcritical tracking), the other with a very high load (critical tracking). The other two tasks placed a high load on short-term memory and attention: one used auditory stimuli, and the other used visual stimuli, and included a difficult motor coordination response with feedback. Preliminary analysis of the data indicated that sustained performance of the tasks induced both behavioral and neurophysiolgical signs of fatigue (Interim Progress Report, 1APR84, Contract F33615-82-C-0628, U.S. School of Aerospace Medicine). The behavioral measures provided a clear indication of intervals during which performance was impaired. Examination of averaged event-related potentials indicated that in the fatigued state the amplitudes of the N2 and P3 peaks were reduced.

Based on these encouraging results, a final paradigm was implemented in which each full fatigue recording consisted of three parts: (1) practice day (4 two-hour task modules), (2) fatigue day (7-8 two-hour task modules), and (3) follow-up day to measure recovery and provide a control for automatization of task performance (3 two-hour task modules). Fifty-one brain potential channels, two eye-movement channels, muscle potentials, respiration and electrocardiogram were recorded. During the last half of 1984 and the first half of 1985, full "fatigue recordings" were made from four Air Force fighter test pilots. (Only 33 brain potential channels were recorded during the

fatigue session on two of the pilots.) Highly sensitive types of neurocognitive pattern analysis (Gevins et al., 1981, 1983, 1984a,b, 1985), which may be able to discern predictive indicators of impaired performance, are now being applied to these data.

3. Experimental Protocol. Three United States Air Force test pilots based at Edwards Air Force Base in California, and one USAF test pilot based at Albuquerque, N.M. served as subjects for this study. The mean age of the group was 34 years, with a range of 31 to 39. All subjects were right-handed males in excellent health. The experiment was divided into four recording sessions, conducted over the course of four days. Session One, "Task Acquisition," on the first day, consisted of the pilots performing the experimental tasks for about eight hours, until performance asymptoted. Sessions Two and Three took place on the second day. During Session Two, "Practiced Performance," pilots performed the tasks for about eight hours, and then continued into Session Three, "Fatigue." It consisted of another 6-8 hours of recording, and terminated between 12:25 and 3:20 a.m., when one or both of the following occurred:

(a) Subjects asked to end the session.

(b) Useable EEG data could no longer be recorded because of excessive eye movements or head nodding and drooping.

On the third day no recording was done and subjects were allowed to rest. Session Four, "Overlearned," took place on the fourth day, and consisted of another 6-7 hours of recording in order to measure practice effects.

Recording procedures began at 8:30 A.M. Orientation, electrode application and position measurement, system checkout and calibrations took about 3 hours. The experiment was conducted in an acoustically dampened, air-conditioned chamber; room temperature, lighting, and seating position were adjusted as necessary. Because subjects were seated for long periods during each session (up to 18 hours on Day 2), all possible efforts were made to ensure their continuing comfort. Subjects were brought water and permitted to stretch at regular intervals. They were allowed to drink coffee or soft drinks during the day and with dinner; after dinner only non-caffeinated drinks were provided for all but one subject. The experiment consisted of five different tasks: (1) the Visuo-Motor Monitoring Task, null memory condition (VMMT 0-back); (2) the Visuo-Motor Monitoring Task, memory load condition (VMMT 2-back); (3) an Auditory Monitoring Memory (AUM) Task; and the (4) Sub-critical and)5) Critical Tracking Tasks (Allen & Jex, 1971; Jex, 1978). Recording sessions began and ended with the Tracking Tasks. In between, the other three tasks were organized into sorties, consisting of 100 to 300 trials of each type. Table 1 shows a typical sortie for sessions 1, 2 and 4. Session 3, "Fatigue," differed in two ways: (1) it did not include the 0-back VMMT task, and z92) an easier version of the VMMT 2-back task was used during the later part of the session when the subject's performance was declining significantly.

All four recording sessions began and ended with the critical and sub-critical tracking tasks (CTT/SCT), except Session 3, where they

Table 1

Typical "sortie" for sessions #1, 2 & 4

VISUO-MOTOR MONITORING TASKS:

NO MEMORY LOAD (0-back), 200 TRIALS (30 min.)
MEMORY LOAD (2-back), 300 TRIALS (45 min.)

AUDITORY MONITORING TASK, 150 TRIALS (15 min.)

TRACKING TASKS (15 min.)

were also included in the middle. In between the tracking tasks, the VMMT 0-back, VMMT 2-back, and the AUM tasks alternated. For these three tasks, sorties consisted of two or four 50-trial blocks for the 0-back (null memory) task, three or six blocks of 50 for the 2-back (memory load) task, and three blocks of 50 for the AUM task. Each block was self-initiated by the participant.

The AUM task consisted of one memory condition: three-back memory load. In this task, the pilots were asked to respond whenever the current stimulus was the same as the number three back. Stimuli consisted of single-digit numbers from 0 to 9 generated by a Votrax speech synthesizer (duration from 245 to 430 msec), and presented in blocks of 50. The interstimulus interval varied randomly from 4 to 5 seconds. Stimuli were presented over two speakers, located in front of the pilots; as in the VMMT, pilots responded by pressing on a force transducer with the forefinger of their right hand. In the AUM task, unlike the VMMT, the response registered as either on or off, and there was no feedback or warning signal for individual trials. Subjects did receive feedback at the end of each block of trials, showing:

(a) Targets (catch-trials) hit.

(b) Targets missed.

(c) False positives.

(d) Average reaction time.

(e) Standard deviation of reaction time.

The tracking tasks were developed for research to measure psychomotor skills vital to a broad class of tasks likely to be performed in space (Jex, 1978; Allen & Jex, 1971). Both the Critical and Sub-critical tracking tasks required the pilot to control the motion of a luminous horizontal CRT line with an isometric (force) control stick. As the dynamically unstable horizontal line fell off from a reference point in the center of the screen, the pilot applied compensatory pressure on the control stick. Difficulty in the SCT task was held constant at a level which the pilot could maintain for 10 minutes. In the CTT the instability of the line steadily increased at a pace which brought loss of control in one to two minutes. CTT trials ended when control was lost. Ten minutes of SCT were followed by five CTT trials.

4. Detailed Description of VMMT Task. The VMMT was designed to allow precise control of stimulus parameters, motor activity and eye movements. This was done by combining the numeric judgment task used previously (Gevins et al., 1981) with a memory element based on the "delayed digit cancelling task." Stimuli consisted of single-digit numbers (325 msec duration) presented on a Videographics-II amber CRT monitor 70 cm from the subject. Stimuli subtended a visual angle under 1.5 degrees, with an illumination of 0.5 log fL against a background of -1.5 log fL. Subjects responded on each trial with a ballistic contraction of their right index finger on an isometric force transducer with a force proportional to the stimulus number on a linear scale from 1 to 9. A 2-digit feedback number (325 msec

duration) indicating the exact force applied to one-tenth of a unit was presented 1 sec after peak response pressure. The inter-trial interval was 1.8 sec, during which a fixation symbol (X) was on the screen. To rule out the possibility of memorization of stimulus sequences across the series of recording sessions, 5 different series of 150 stimuli for the 2-back and 5 series of 100 stimuli for the 0-back task were formed from random-number tables. In order to dissociate motor and memory errors in move trials of the 2-back memory task, the stimulus numbers were chosen so that the two numbers held in memory and the current stimulus number were all at least two digits apart (e.g., 5-7-3). (The Fatigue session used different sequences where the numbers were at least three digits apart because of the degraded level of motor control.)

The feedback number was underlined if the response was sufficiently accurate. Accuracy was based on an adaptive error tolerance, the geometric average of the error (the distance from the required response pressure) on the previous 5 move trials (Gevins et al., 1981, 1983). Move trials falling within the adaptive error tolerance were termed "win" trials. This adaptive error tolerance served to equalize task difficulty across the session and to indicate the current performance trend. The timing of a 2-back memory trial is illustrated in Table 2. After each 50-trial block, summary performance statistics were presented on the video screen. These were:

(a) Average movement force error (difference from required pressure) and its standard deviation.

(b) Average adaptive error tolerance (running mean of previous five trials) and its standard deviation.

(c) Average response time and its standard deviation.

(d) The number of target trials (catch trials) presented, and the number missed (false positives).

(e) Number of time outs (no response within set period).

The two memory load conditions in the VMMT were: a null memory or 0-back condition, in which the required response pressure was indicated by the current stimulus number; and a 2-back memory condition, in which the response pressure was indicated by the stimulus number two trials back. In order to add a recognition element to the tasks, and also to avoid overly short response times in the memory task, 20% of the trials in both conditions were designated as catch-trials; subjects were required not to respond during those trials. As shown in Table 3, in the 0-back condition, these no-move catch trials were those where the stimulus number was 0; in the 2-back condition (Table 4), catch trials were designated as the occurrence of a stimulus number identical to the 2-back stimulus number.

The difference between the 0-back and 2-back tasks was the use of short-term working memory to maintain the two constantly changing numbers and recognition of the 2-back identical numbers which were the no-move "targets" in the memory task, in contrast to the immediate response to current stimulus numbers and recognition of the number "0" which was the only no-move target in the non-memory task.

Table 2

Timing of a 2-back VMMT trial. An "X" appears on the screen between trials. At the beginning of the trial, the "X" is turned off (XO). The stimulus number then appears (S), followed by the response (R). After the response, the feedback (F) appears. At the end of the trial, the "X" reappears (X).

Event:	XO	S	R	F	X
Time:	(0)	(0.75)	(1.25)	(2.75)	(4.00) (secs)

Table 3

0-BACK (NO MEMORY) VMMT TASK: Typical sequence of 6 trials. "N" indicates no response movement.

STIMULUS:	4	1	9	0	7	3
RESPONSE:	4.6	2.0	8.9	N	6.1	3.4
FEEDBACK:	4.6	2.0	8.9	OK	6.1	3.4

Table 4

2-BACK (MEMORY) VMMT TASK: Typical sequence of 6 trials at beginning of block. "N" indicates no response movement (catch trial).

STIMULUS:	3	7	6	9	6	2
RESPONSE:	N	N	3.7	7.2	N	8.9
FEEDBACK:	OK	OK	3.7	7.2	OK	8.9

It is assumed, of course, that accurate ongoing motor performance in both tasks required maintenance of a motor "memory" and its adjustment in response to feedback. In the memory task, except for the first 2 trials of a block where no response was required, each trial required: (1) judgement of whether the current stimulus number matched the 2-back number and withholding response if it was (no-move trials, quasi-random 20%); (2) execution of a precise pressure corresponding to the 2-back number if it did not match the current stimulus (move trials, 80%); (3) deletion of the 2-back number from memory, and maintenance of the 1-back number, storage of the current stimulus number and their order; and (4) evaluation of the feedback number in order to maintain accurate motor performance. The latter operation could involve interference between the stored numbers and the feedback number. Trials averaged about 6 seconds in length; the time between presentation of a stimulus number and response to that number in the memory task was about 12 seconds. It was found that this pace was fast enough to allow maintenance of the numbers in short-term memory without rehearsal. Participants commonly reported that they developed a "sense" for the 2-back number (although one person reported a visual strategy) sufficiently accurate to permit response pressures to be almost as accurate as the non-memory task. Also, some persons developed faster response times in the memory task during the course of the recording sessions, yet exhibited no deficiency in detection of no-move stimulus matches. This suggests a priming of the motor system (since the relevent 2-back number is known), with the ablity to abort this preparatory facilitation upon recognition of a 2-back match.

5. Recording Methods. Fifty-one EEG channels, referenced to A2, were recorded. The montage is shown in Figure 10. Recordings of the first two subjects, made during the transition period from 26 to 51 channels, were made with a 33-channel montage which had sparser coverage over the top of the head and fewer electrodes at the periphery. Vertical and horizontal eye movements from electrodes above and below one orbit and at outer canthi were also recorded, as were the responding flexor digitori muscle potentials and output of the response force transducer. A1, EKG and respiration were also recorded. Brain potentials were recorded with an Electrocap International nylon mesh cap using tin electrodes and $SnCl_2$ electrolyte gel, amplified by a 64-channel Bioelectric Systems Model AS-64P with .016 to 50 Hz passband and digitized to 11 bits at 128 Hz. All signals were monitored on 3 8-channel and 2 16-channel polygraphs.

Table 5 gives an overall picture of a typical recording. Table 6 shows in more detail the second, or fatigue, day, including the pilots' self report of fatigue, which was requested periodically. Subjective Fatigue was measured on a 7-point scale (Crew Status Survey, USAF SAM-202).

6. Formation of Data Sets. Polygraph records were edited off-line by two independent raters to eliminate trials with evidence of eye movement in the EOG channels and muscle or instrumental artifacts in the EEG channels from three-quarters of a second before the stimulus to one and one-quarter seconds after the end of the feedback. Move trials where response movement was not unimodal and ballistic, or not made within 1.25 seconds after the stimulus, were eliminated. No-move trials where movement occurred were eliminated. Data sets were pruned of outliers for EOG, EMG and behavioral variables such as move velocity and acceleration.

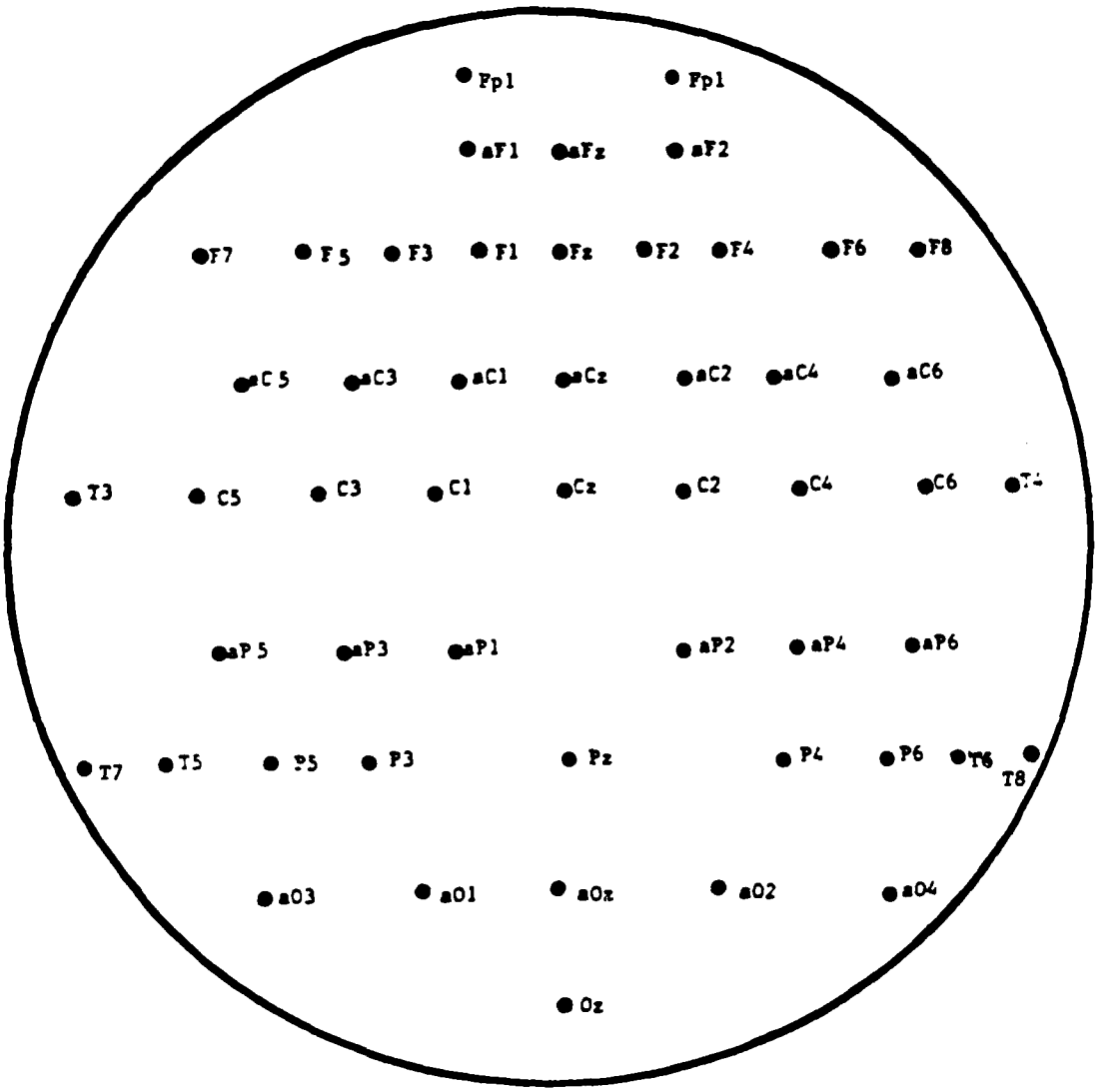

Fig. 10. Electrode Montage for Fatigue Experiment.

Table 5

FATIGUE EXPERIMENT

PILOT: HW

DATE	SESSION	TIMES OF DAY	DURATION (HOURS)
23 APR 85	1 (LEARNING)	11:25 - 19:15	7:50
24 APR 85	2 (PRACTICED)	11:25 - 19:10	7:45
24 APR 85	3 (FATIGUED)	20:20 - 02:25	6:05
26 APR 85	4 (OVER-LEARNED)	12:10 - 18:05	5:55

Table 6

FATIGUE DAY

24 APR 85

PILOT: HW

	TIME OF DAY	ELAPSED TIME (HOURS)	SUBJECTIVE FATIGUE
SESSION 2			
Sortie 1	11:25 - 13:15	1:50	3
LUNCH			
Sortie 2	14:25 - 15:35	4:10	3.5
Sortie 3	15:44 - 17:20	5:55	4.5
Sortie 4	17:33 - 19:10	7:45	5
DINNER			
SESSION 3			
Sortie 1	20:20 - 22:55	11:30	5.5
Sortie 2	23:01 - 00:15	12:50	7
Sortie 3	00:23 - 01:25	14:00	7
Sortie 4	01:29 - 02:25	15:00	7

Session 3 terminated when participant began falling asleep.

Fatigued and rested data were selected based on reaction time and error. For Pilot HW, nine blocks of 2-back data (450 trials), recorded between 12:41 and 02:25 and having the highest error and longest reaction times, were selected as representative of the fatigued state. Nine blocks with the lowest mean reaction time and error, recorded between 14:25 and 16:30 were chosen from Session 2 for alert data. After editing, there were 380 trials from Session 3, and 273 trials from Session 2. As shown in Fig. 11, performance degraded consistently as participants fatigued. Reaction time and error increased, even as trials became subjectively easier to perform due to the adaptive error tolerance algorithm.

7. Preliminary Analysis. Preliminary analyses have been completed on the practiced data of three pilots and the fatigued data of two pilots. In the alert condition, in a pre-stimulus anticipatory interval, delta-band filtered data revealed striking, localized differences between conditions with a low and high load on short-term working memory. In a 375-msec wide interval centered 375 msec before the stimulus, strong covariances between a left anterior frontal and left superior temporal, right anterior frontal and right premotor electrodes distinguished the high memory load from the low memory load. In the pre-stimulus, high-memory load interval of the fatigue condition, the covariances were reduced in number and greatly weakened.

V. RECENT DEVELOPMENTS IN NCP ANALYSIS

A. Data Collection

1. 64-channel EEG Recording Technique and Automated Artifact Rejection. Recording capacity has recently been expanded to a full 64 EEG channel capacity to provide uniform scalp coverage with an inter-electrode distance of about 3.25 cm (Fig. 12). All recordings are referenced to one mastoid (usually A2); the other (A1) is recorded as a separate channel so that a laterally balanced (A1+A2) reference may be computed off-line, avoiding the undesirable boundary condition on the potential field created by linked-ear references. Signals are digitized at 12 bits full scale at 256 samples/sec, and stored on magnetic tape by the PDP11-60. Forty-eight of the 64 channels are monitored at a time for electrode problems. Improved automated artifact rejection algorithms using statistical pattern recognition to combine amplitude, frequency, and topographic features (Morgan & Gevins, In prep.) are applied off-line. These algorithms satisfactorally perform a preliminary data screening.

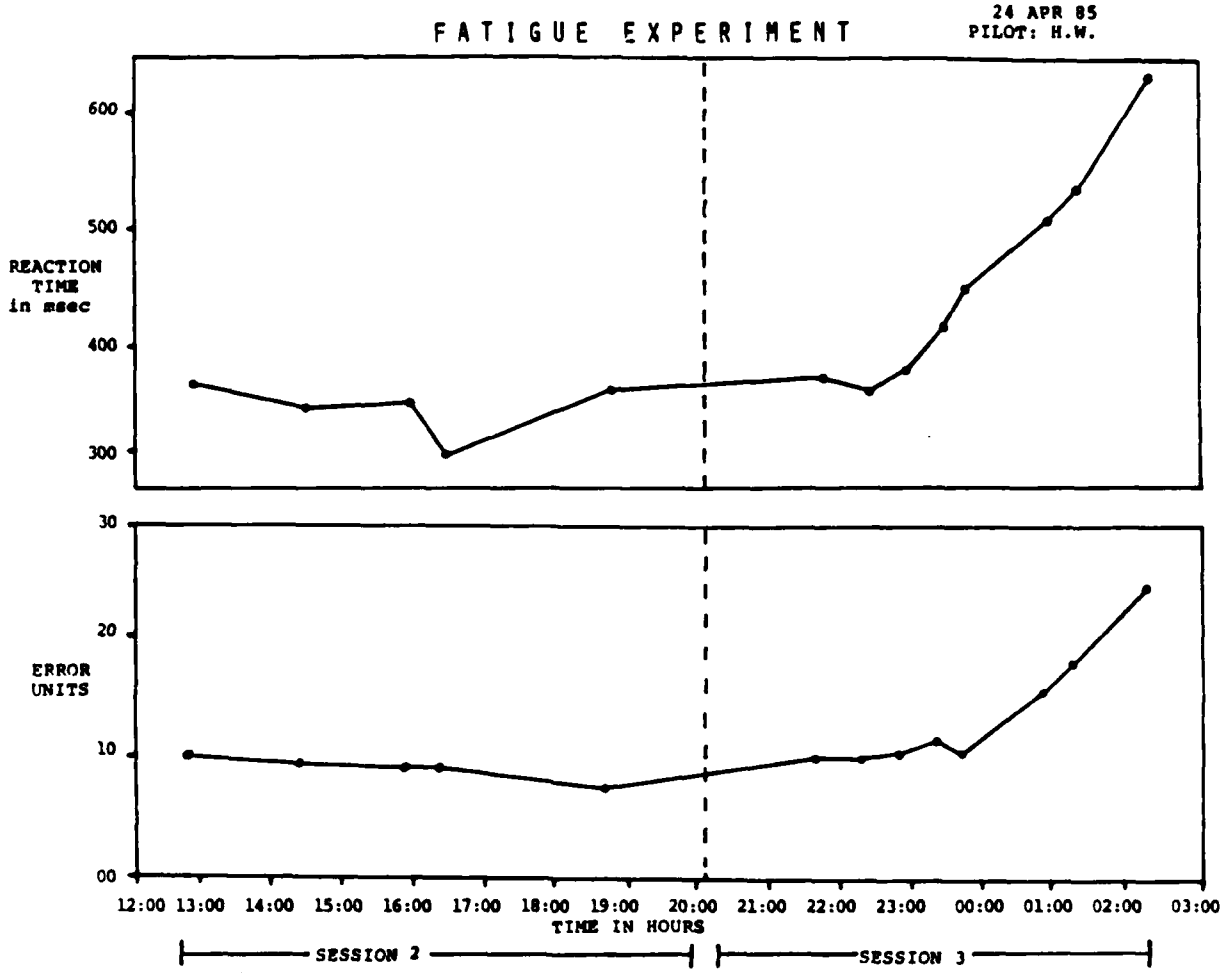

Fig. 11. Performance degradation shown as participants fatigued.

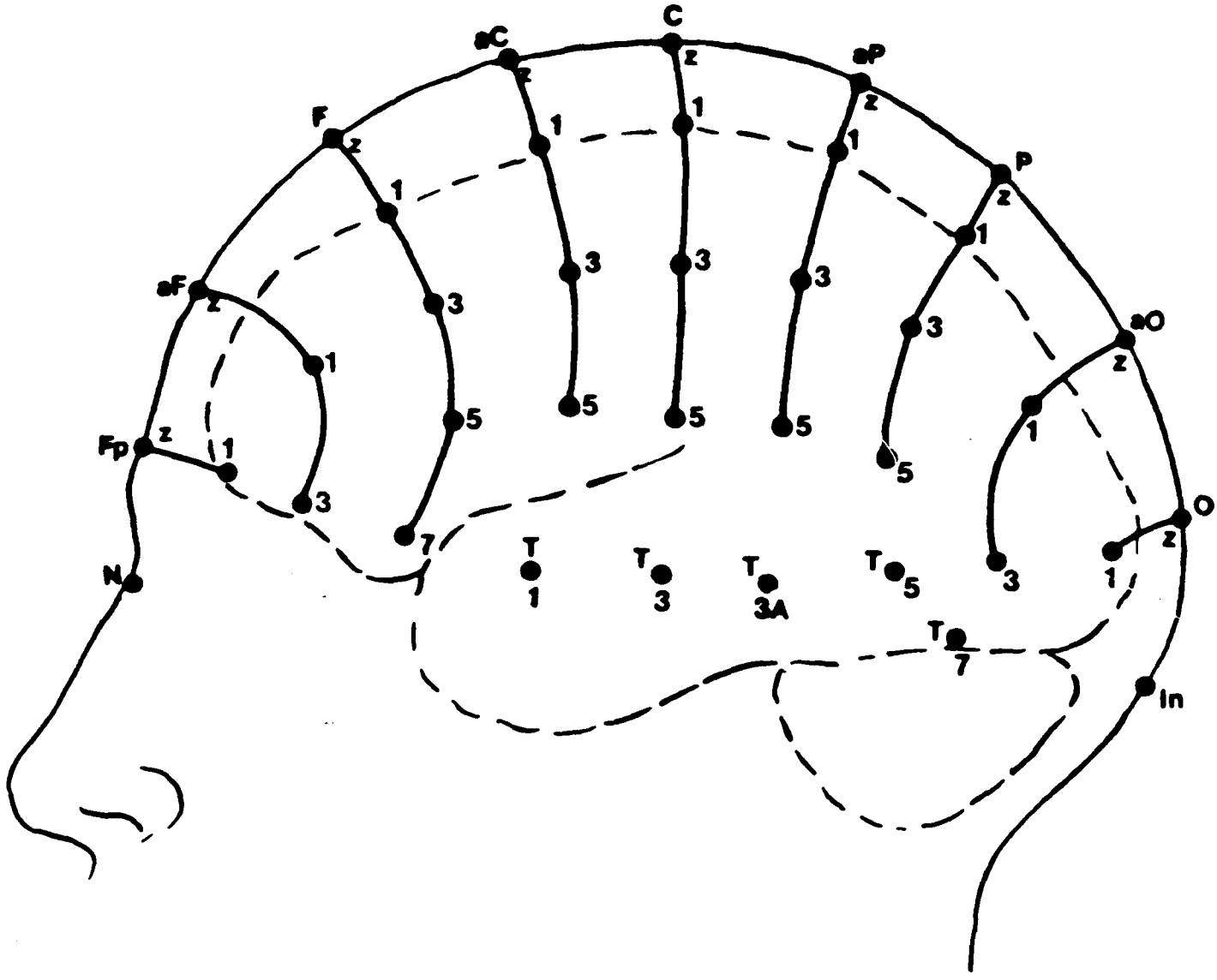

Fig. 12(a). Expanded 10-20 System of electrode position nomenclature. Additional coronal rows of electrodes, interpolated between the International 10-20 System coronal rows, have the letter a for "anterior" added to the designation for the next row anterior, e.g., aPz for anterior parietal midline electrode. With 64 electrodes, the average distance between electrodes on an adult head is ~3.25 cm.

Fig. 12(b). Participant wearing 64-channel EEG recording cap.

Statistical pattern classification techniques were used to evaluate the performance of two eye movement artifact removal techniques: Amplitude Subtraction Eye Movement Correction Procedure and Spectral Subtraction Eye Movement Correction Procedure (Fig. 13). Although visual comparison showed both methods to be effective, the objective evaluation technique suggested that the frequency-dependent system identification method may sometimes be more effective for eye blink removal.

2. Digitization of Electrode Positions. Before and after a recording session, the position of the external center of the grommet of each electrode is measured in three dimensions using a 3-D digitizer (Fig. 14). The participant rests his head in a padded stabilizing jig for the 5 minutes required to digitize the positions of all electrodes. Correction to scalp positions is made by a least-squares fit Multiple Linear Regression, which yields the general ellipsoid surface best fitted to the set of digitized positions, and the digitized coordinates are translated to a coordinate system centered on this ellipsoid.

3. MRI Imaging for Determining Positions of Electrodes and Cortical Structures. Full sets of Magnetic Resonance Images (MRI; Fig. 15) are made at UCSF Long Hospital facility. These are high-resolution (0.8 mm pixel) 3-axis cross-section images of soft tissue 1 cm apart over the whole volume of the head. The pictures are digitized to give coordinate surfaces for scalp, outer and inner skull surfaces, and cerebral surface, including loci of major fissures. Comparison of electrode positions and MRI measurements provides correlation of electrode positions and cortical areas, allowing comparison of functional neuroanatomy across individual participants for localized sensory and motor cortical ERP components. The direct measurements of thickness of scalp and skull provides accurate information for use in spatial deconvolution (see below).

B. Data Analysis

1. Trial Selection Using Pattern Recognition. A great deal of effort has been expended in attempts to form improved estimates of the averaged ERP (reviews in McGillem et al., 1981, 1985; McGillem & Aunon, in press; de Weerd, 1981; Gevins, 1984). Most methods assume that task-related signals are present in every trial and also have inherent assumptions about the statistical properties of signal and noise. We have developed a method for ERP estimation without the first assumption and with a relaxed second assumption. To do this, separate averages are formed from trials which are correctly or incorrectly classified by a statistical pattern recognition procedure. In the averages of correctly classified trials, the ERP peaks are enhanced in comparison with the original averages. The averages of incorrectly classified trials resemble the background EEG.

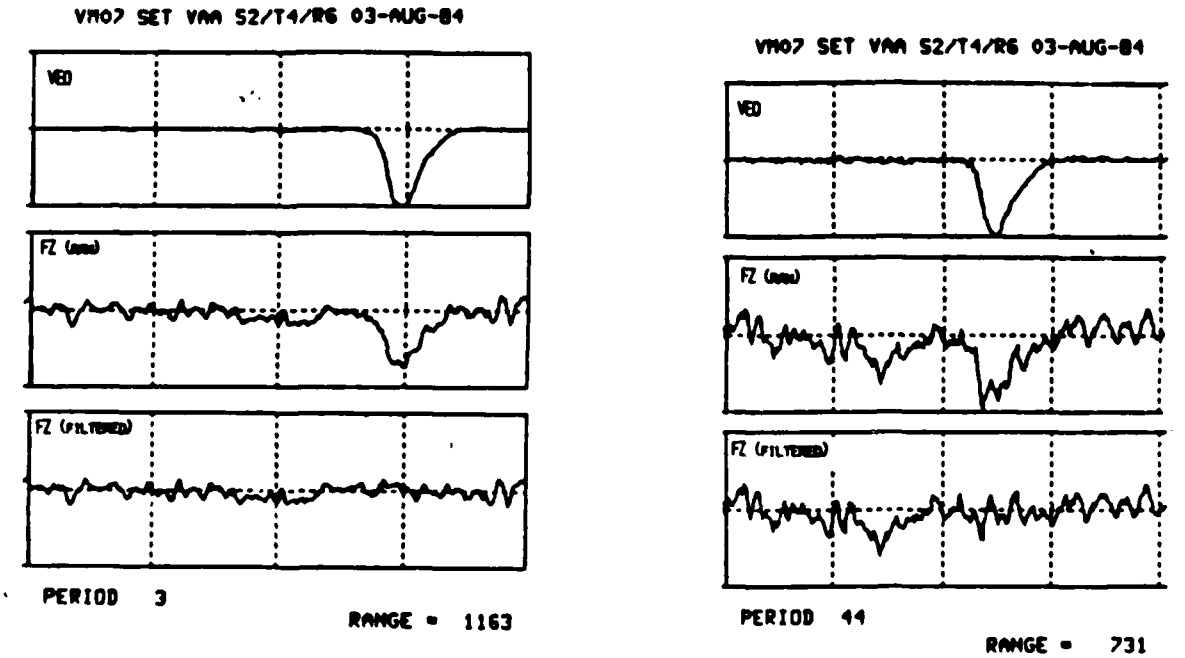

Fig. 13. Examples of application of the spectral eye-movement filter to large blink artifacts. [After Gevins et al., 1984b.]

Fig. 14. Technician digitizing positions of scalp electrodes. The measurements take about 5 minutes.

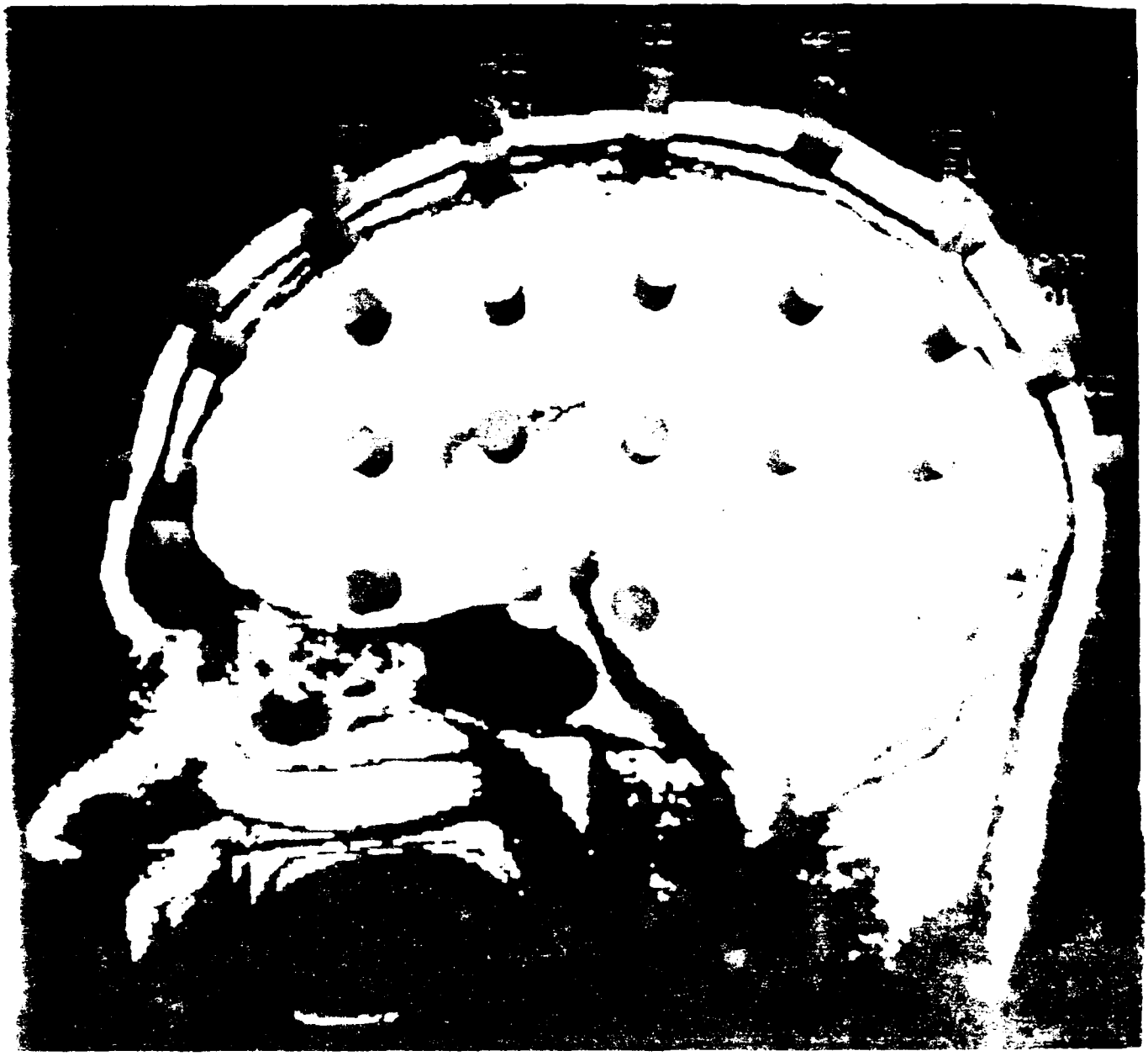

Several dozen applications of this technique suggest that it is successful in identifying trials with a poor signal-to-noise ratio, and provides a simple method of ERP estimation with minimal a priori assumptions about the characteristics of the signal.

2. Wigner (Time-Frequency) Distributions. The ERP waveform is a function of time and does not provide explicit frequency information. Power spectra of ERP waveforms provide frequency information but obscure time-dependent phenomena. A view of the spectrum as it changes over time would give a new view of the evolution of different frequency components of the ERP. A simple approach would be to compute the spectrum over highly overlapped windows of the average ERP. However, such a "spectrogram" would smear together events within each analysis window. While there is an unavoidable trade-off between frequency and time resolution (known as the Heisenberg Uncertainty Principle), the spectrogram is an inflexible way of determining this choice.

A preferred method is to compute a general function of time and frequency called the Wigner Distribution (Claasen & Mecklenbrauker, 1980; Janze & Kaizer, 1983) which approximates the instantaneous energy for a given time and frequency. In practice, the "purified" ERPs (obtained using the procedure above) show strong enough energy "peaks" in the Wigner Distribution to validate very simple interpretations of the time and frequency locations of signal energy. The Wigner Distributions are being used to determine digital filter characteristics which produce optimal time-frequency resolution for a given data set.

3. Balancing Data Sets. Special attention is given to the preparation of data sets, since we believe that this is a highly neglected aspect of experimental control. In order to form balanced pairs of data sets for each neurophysiological hypothesis, the total set of artifact-free trials from each recording is submitted to an interactive program (ADISORT) which displays the means, t-tests and histogram distributions of about 50 behavioral and other variables. Pairs of data sets can be quickly inspected for significant differences in variables not related to the hypothesis and pruned of outlier trials until balanced, usually to a conservative alpha of .2. The ADISORT program greatly facilitates the handling of large amounts of data and permits a high degree of control of stimulus, behavioral and other variables which would not otherwise be possible. It outputs labeled lists of trials which vary only according to the chosen hypothesis to be submitted to the signal processing and analysis programs of our system. Variables include stimulus parameters, responding finger, response onset and inter-movement times, response movement force, velocity, acceleration and duration, error and adaptive performance measure. There are also indices of eye movement, EMG activity and "arousal," which are measures of integrated energy in the vertical and horizontal EOG channels, the EMG channel and the Pz electrode, respectively, computed in separate 500-msec epochs before and after the onset of cue, stimulus, response and feedback.

4. EEG Spatial Signal Enhancement. Electrical currents generated by sources in the brain are volume conducted through brain, cerebrospinal fluid, skull and scalp to the recording electrodes. Because of this, potentials due to a localized source are spread over a considerable area of scalp, so that the potential measured at a scalp site represents the summation of signals from many sources over

much of the brain. (We have estimated the "point spread" for a radial dipole in the cortex to be about 2.5 cm --- Fig. 16). This spatial low-pass filtering makes source localization difficult, even for cortical sources, and causes the potentials from local sources to be mixed with those from more distant generators. By modeling the resistive properties of the tissue between brain and scalp surface, we can perform a deconvolution of the potential to the level of the brain surface without imposing assumptions as to the actual (cortical or sub-cortical) source locations. This technique is being evaluated, along with the local Laplacian operator (or "Hjorth montage").

(a) Laplacian Operator. Poisson's equation states that the Laplacian of the potential is proportional to the local density of current sources. An estimate of the average Laplacian over a volume of scalp surrounding a given electrode will then be proportional to the net current leaving that volume. The 2-dimensional Laplacian in the plane of the scalp is proportional to the net current through the edges of the volume. Since there are no current sources in the volume, this net current is equal to the local density of current flow up through the skull (local current source density or CSD) (Hjorth 1975, 1980, 1982; Thickbroom et al., 1984 --- Fig. 17b). [Note that this term does not refer to neuronal sources, but only to local current emerging from the skull.]

This transform has a localizing effect since it is relatively insensitive to sources beyond the proximal electrodes, and has the advantage of being independent of reference electrode site. The usual implementation (Hjorth, 1980; Thickbroom et al., 1984) estimates the Laplacian operator L_k at a given electrode k as an average of the directional derivatives from each surrounding electrode i to the given electrode k:

$$L_k = \frac{\sum_{i \neq k} (V_k - V_i) / R_{ik}}{\sum_{i \neq k} 1 / R_{ik}}$$

where V_i are the potentials at the respective electrodes and R_{ik} are the distances separating the electrodes. This quantity is proportional to a second-difference estimate of the Laplacian for a "rosette" of electrodes uniformly surrounding the given electrode (Hjorth, 1975), with the factor of proportionality being a geometrical factor (the electrode separation squared), but departs from the same proportionality as the configuration of electrodes departs from the symmetrical, notably when all the proximal electrodes are on one side of the given electrode. We have improved upon the conventional method of Hjorth (1975) by using actual measured interelectrode distances. However, we have been unable to overcome the difficulties associated with the Laplacian computation for peripheral channels, and do not include them in analysis.

(b) Spatial Deconvolution for Reducing the Effect of Volume Conduction. Spatial deconvolution is the modeling of the propagation of electric potentials from brain to scalp. The simplest analytic deconvolution approach is to represent the tissue between brain and scalp electrodes as concentric spheres with different resistivities (Fig. 18). The form of the potential wherever

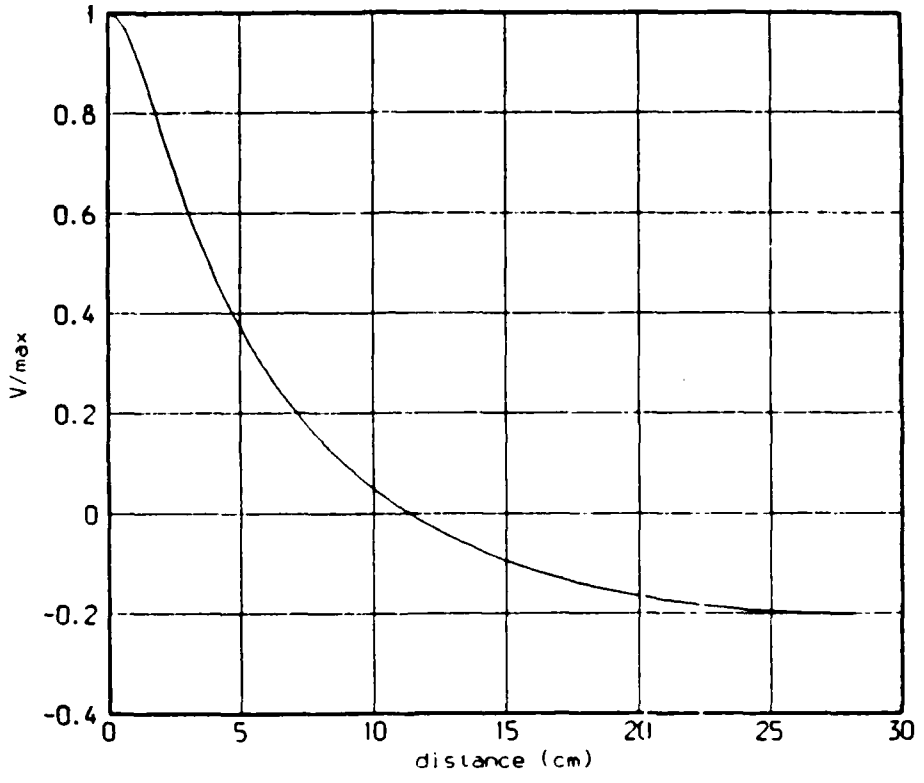

Fig. 16. Point Spread Function. Distribution of potential at the scalp in a 3-shell model of the head produced by a single radial dipole in the cortex as a function of distance in cm from the scalp site point overlying the dipole. The tissue between the cortex and scalp act as a spatial lowpass filter which blurs the potentials at the scalp. Spatial deconvolution attempts to remove this blurring.

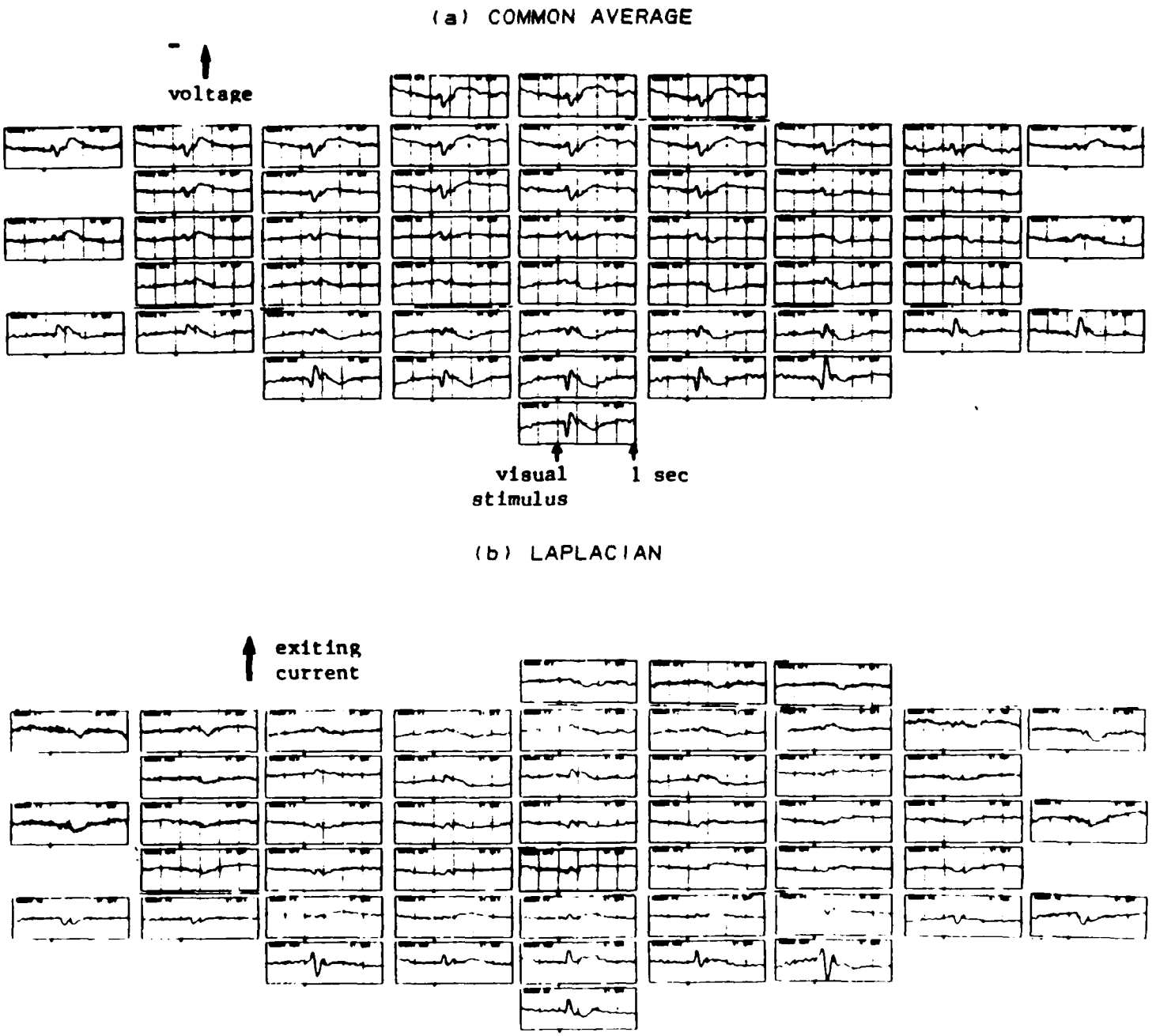

Fig. 17. Three representations of averaged stimulus-locked event-related waveforms for visual move trials from participant AV07. Fifty channels. (a) Common Average Reference. (b) Laplacian (second spatial derivative of potential field).

DECONVOLVED

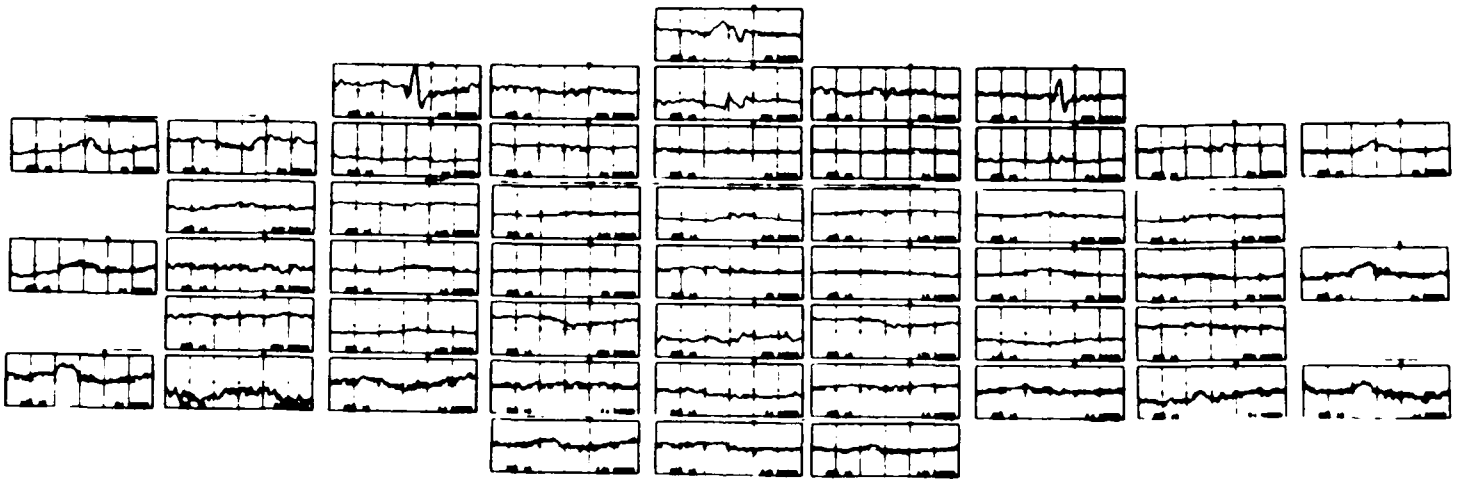

FIG. 17(c). Spatial Deconvolution.

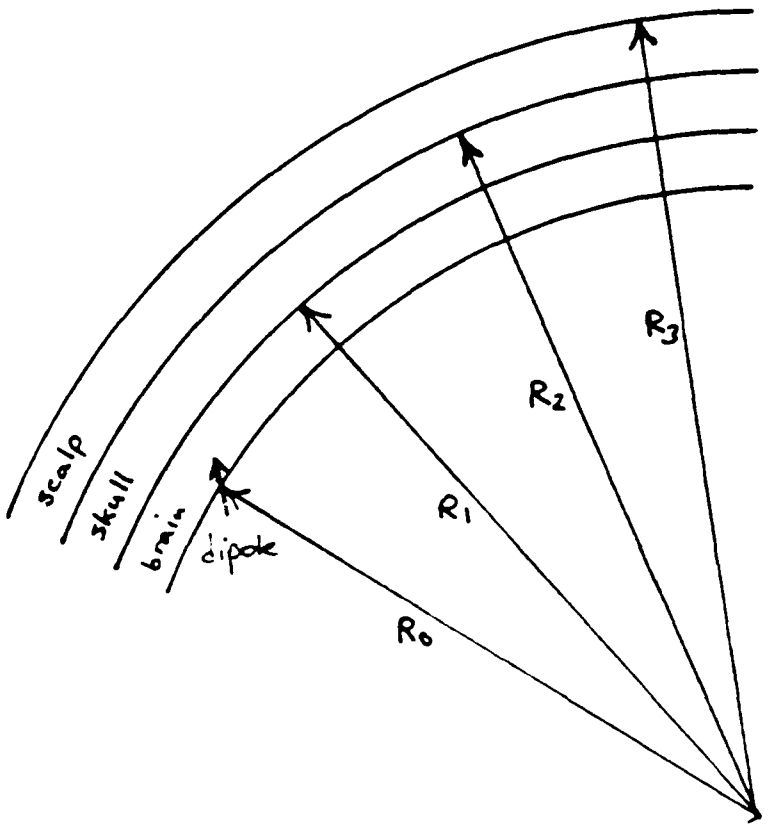

Fig. 18. Three-concentric sphere model used for modeling volume conduction effects on brain potentials.

there are no sources is represented as the general solution of Laplace's equation in spherical polar coordinates:

$$\Phi_i = \sum_{n=0}^{\infty} \sum_{m=-n}^{n} \left\{ A_{inm}\, r^n + B_{inm}\, r^{-(N+1)} \right\} Y_{nm}(\theta,\phi) \qquad (1)$$

where the spherical harmonic functions $Y_{nm}(\theta,\phi)$ which contain all the angular dependence of the potential, are solutions of Laplace's equation forming a complete orthonormal basis on the unit sphere, and the A's and B's are coefficients to be determined from the boundary conditions. At each interface of different media, the potential and the current normal to the surface must be continuous:

$$\Phi_i \Big)_{R_i} = \Phi_{i+1} \Big)_{R_i} \qquad (2)$$

$$\sigma_i \frac{\partial \Phi}{\partial r} \Big)_{R_i} = \sigma_{i+1} \frac{\partial \Phi_{i+1}}{\partial r} \Big)_{R_L} \qquad (3)$$

where R_i is the radius of the boundary between media i and i+1, and where the σ_i are the conductivities of the respective media. These boundary conditions constitute a series of equations which may be solved in several ways: to represent the coefficients in the expansion of the electrical potential at the surface of the scalp, in terms of the coefficients in the expansion at the surface of the brain, or in terms of a distribution of dipole sources at some level in the cortex. The potential at the scalp is then represented as a sum (convolution) over cortical sources or potential distributions, and inversion of this relation (deconvolution) allows one to represent the sources (cortical potential coefficients) in terms of the measured potentials.

This procedure is independent of hypotheses about the character, position, or orientation of the neuronal sources of electric potential other than that the tissue intervening between brain and scalp are free of any active sources. In practice, the thicknesses of scalp and skull at each electrode position are measured from the MRI images of each person. The CSF shell has been omitted in our initial studies, following the results of the Cal Tech Group (Ary et al., 1981; Kavanagh et al., 1978; Darcey et al., 1980). We are experimenting with methods of measuring the conductivities of the layers.

Several recordings of an auditory-visual (AV) task were made with 50 scalp channels during the summer of 1983. The positions of electrodes were digitized using a stereophotogrammetry system developed for craniofacial research (Baumrind & Curry, 1984; Curry et al., 1982).

(This has since been replaced by direct digitization of the electrode locations.) The digitized positions were used to implement the transformation by the Laplacian operator and a form of the spatial deconvolution modeling in terms of a distribution of radial dipoles over the cortex in a 4-sphere model of the head (cerebrum, cerebro-spinal fluid, skull, and scalp).

The Laplacian estimate at each electrode was computed as the average of the directional derivatives from adjacent electrodes (Figs. 17b & 19b). The deconvolution model represents the scalp-recorded potential distribution as deriving from a distribution of radial dipoles in the cortex (Figs. 17c & 19c). In order to assess the reduction in interelectrode correlation due to volume conduction, we have calculated the interelectrode correlation over the stimulus-locked visual ERP for each pair of channels for the common average reference, Laplacian, and deconvolved ERPs. Then, using the measured electrode positions and the 4-sphere model of the head, we calculated the point spread for each pair of electrodes. A linear regression of correlation versus point spread reveals the degree of association for the common average derivation. The same regression for the Laplacian and deconvolved derivations shows the degree of association to be more reduced for the deconvolution than for the Laplacian (Table 7).

The spherical model of the head is not, of course, a realistic representatin of the true geometry of an individual's head and brain. The temporal areas are particularly problematic because of their relative flatness. We are formulating a more realistic model using finite-difference representations of the electrical properties of the tissue intervening between the cortex and the surface and the scalp. The key to this method is the availability of structural information about each participant's brain, skull and scalp from the Magnetic Resonance Image (MRI).

5. Source Localization. Given an adequate model of the tissue of the head, a knowledge of the positions, multipole character, orientations, and magnitudes of the sources of the brain electrical potential and magnetic fields suffices to determine the measured potentials and fields at the scalp (Plonsey, 1969; Nunez, 1981). Since the potentials may be considered quasi-static (Plonsey, 1969), the spread of potential is governed by Poisson's equation,

$$\nabla \cdot (\sigma \nabla \Phi) = I_v$$

where Φ is the potential, σ is the conductivity tensor, I_V is the volume current source density. Note that the conductivity is, in general, a tensor quantity, which may reflect different conductivities in different directions (anisotropy), and a function of position. We will consider only isotropic models, however, in regions free of sources, and this reduces to Laplaces' equation,

$$\nabla \cdot (\sigma \nabla \Phi) = 0 \quad ,$$

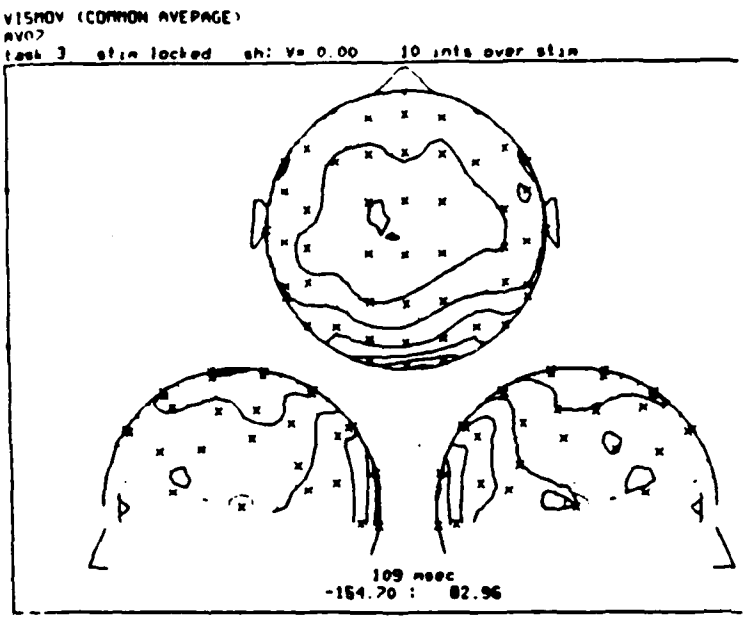

(a)

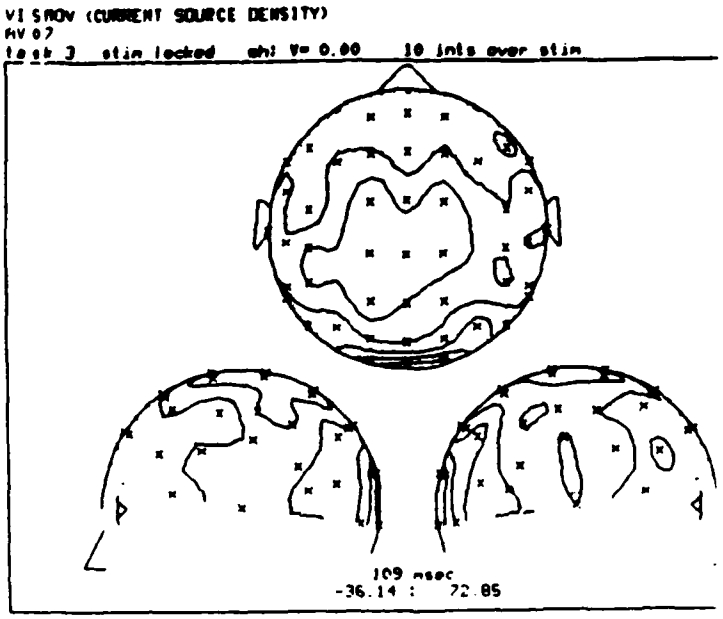

(b)

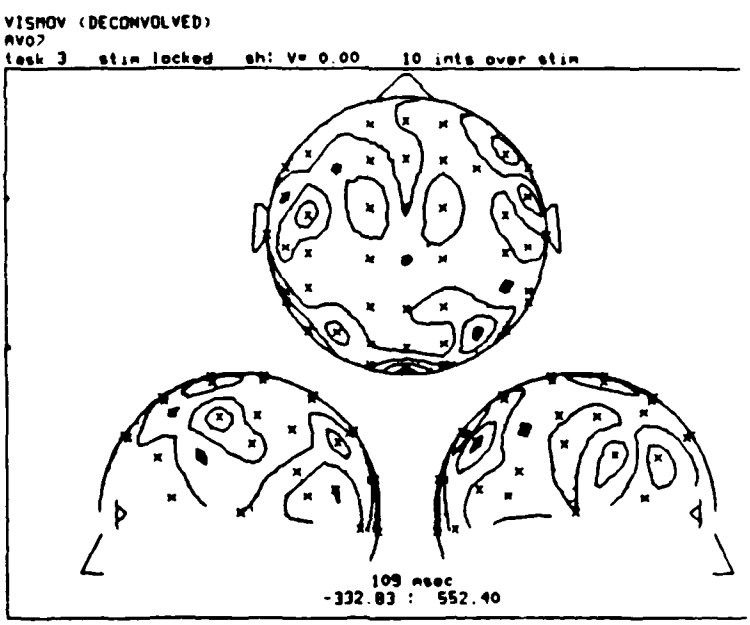

(c)

Fig. 19. Contour plots of event-related waveforms of Fig. 18 at 109 msec after the stimulus. There is increased spatial detail with the application of the Laplacian operator, and a further increase with application of the spatial deconvolution. (a) Isopotentials from Common Average Reference. (b) Isocurrent Contours from Laplacian. (c) Iso-dipole Strengths from Deconvolution.

Table 7

Interelectrode Correlation (1) regressed vs point spread function.

SPATIAL OPERATOR	Slope	Intercept	F-ratio (2)
Common Average	0.8878	-0.2644	1278.42
Laplacian	0.3742	-0.1200	251.83
Deconvolution	0.3055	-0.1002	184.61

(1) Interelectrode correlations calculated over stimulus-locked average from 0.5 sec before to 1.0 sec after stimulus.

(2) Ratio of regression to residual variance, df = (1,1223).

Unfortunately, a knowledge of the potentials and fields at the scalp does not suffice to determine the sources; a given distribution of potential (field) at the scalp (or any other surface, including the sources) may be produced by infinitely many different distributions of sources. In order to resolve this ambiguity some additional information as to the character, orientation, and/or number of sources must be added to determine the sources of a given potential (field) distribution. One convenient approach which has been successfully applied both to potentials and fields is to model the sources as one or a few equivalent current dipoles whose positions and orientations are unconstrained in a concentric-sphere model of the tissue. This has been applied to averages of sensory ERPs in some situations (Brazier, 1959; Geisler & Gerstein, 1961; Hosek, 1970; Kavanagh, 1972; Ary, 1976; Kavanagh et al., 1978; Darcey et al., 1980) and to averages of ERFs (reviewed in Williamson & Kaufman, 1981a,b; Erne et al., 1981; Williamson et al., 1983; Okada, 1983; Weinberg et al., 1985; Williamson & Kaufman, In press). However, while one or two equivalent current dipoles may be adequate to model the major source of a sensory ERP peak, such models do not seem realistic for even simple goal-directed tasks. Furthermore, the non-spherical topology of the actual anatomy may result in considerable distortion of the results.

More realistic head and brain models, as well as additional information, are required to attempt multi-source localization. We propose a number of steps to achieve these requirements: (1) use of MRI scans and finite-difference models to improve the head and brain model; (2) use spatial deconvolutioon to reduce spatial smearing of potential measures; (3) use of the MEG to provide complementary information; (4) use of other signal processing procedures to enhance the signal-to-noise ratio of both EEG and MEG (such as trial selection and filtering); (5) use of time dependencies as determined from the event-related covariances of fields and deconvolved EEGs to constrain the errors in source modeling; (6) use of several algorithmic approaches, including an exhaustive search for a subset of physical sources from a larger candidate set; and (7) use of PET blood flow data (Budinger et al., 1984) obtained during repetitions of the same task, or a comparable one, from the same subjects to validate the results.

6. MEG Data Analysis. A collaboration is underway with the laboratories of Drs. Williamson and Kaufman, and Beatty. The purpose of this effort is to make a gateway for their MEG data into the ADIEEG system. We are developing special noise suppression digital filters, and will apply our feature extraction and pattern recognition analyses to several data sets.

LITERATURE CITED

Allen, R.W. & Jex, H.R. (1971) Visual-motor response of crewmen during a simulated 90-day space mission as measured by the critical task battery. Systems Technology Inc. Paper No. 100a, May.

Ary, J.P. (1976) The effect of color on localization of the sources of the human visual evoked response. Doctoral dissertation, Ohio State University.

Ary, J.P., Klein, S.A. & Fender, D.K. (1981) Location of sources of evoked scalp potentials: Corrections for skull and scalp thicknesses. IEEE Trans. Biomed. Engr., BME-28, 447-452.

Baumrind, S. & Curry, S. (1984) Merging of data from different records in craniofacial research and treatment. Handbook of the 1984 workshop on non-topographic photogrammetry. American Society of Photogrammetry, July, 35-46.

Brazier, M.A.B. (1959) The historical development of neurophysiology. In H.W. Magoun (Ed.), Handbook of Physiology, 1: Neurophysiology. Washington, D.C., Amer. Physiol. Soc.

Claasen, T.A.C.M. & Mecklenbrauker, W.F.G. (1980) The Wigner distribution --- a tool for time-frequency signal analysis. Phillips J. of Research, 35(3), 217-250.

Curry, S., Moffitt,, F.H., Symes, D. & Baumrind, S. (1982) Family of calibrated stereometric cameras for direct intra-oral use. SPIE Proceedings, 361, 7-14.

Darcey, T.M., Ary, J.P. & Fender, D.H. (1980) Methods for the localization of electrical sources in the human brain. Prog. Brain Res., 54, 128-134.

de Weerd, J.P.C.M. (1981) Estimation of evoked potentials: a study of a posteriori "Wiener" filtering and its time-varying generalization. Doctoral dissertation, Katholieke Universiteit te Nijmegen, The Netherlands, Krips Repro Meppel.

Diewert, G. & Stelmach, G. (1978) Perceptual organization in motor learning. In G. Stelmach (Ed.), Information Processing in Motor Control and Learning. New York, Academic Press, 241-265.

Erne, S.N., Hahlbohm, H.D. & Lubbig, H. (Eds.) (1981) Biomagnetism. New York, Walter de Gruyter.

Geisler, C.D. & Gerstein, G.L. (1961) The surface EEG in relation to its sources. EEG Clin. Neurophysiol., 13, 927-934.

Gevins, A.S. (1980) Pattern recognition of human brain electrical potentials. IEEE Trans. Patt. Anal. Mach. Intell., PAMI-2(5), 383-404.

Gevins, A.S. (1984) Analysis of the electromagnetic signals of the human brain: milestones, obstacles and goals. IEEE Trans. Biomed. Engr., BME-31(12), 833-850.

Gevins, A.S. (In press,a) Correlation analysis. In A. Gevins & A. Remond (Eds.), Methods of Analysis of Brain Electrical and Magnetic Signals: Handbook of Electroencephalography and Clinical Neurophysiology (Vol. 1). Amsterdam, Elsevier.

Gevins, A.S. (In press,b) Statistical pattern recognition. In A. Gevins & A. Remond (Eds.), Methods of Analysis of Brain Electrical and Magnetic Signals: Handbook of Electroencephalography and Clinical Neurophysiology (Vol. 1). Amsterdam, Elsevier.

Gevins, A. & Remond, A. (Eds.) (In press) Methods of Analysis of Brain Electrical and Magnetic Signals: Handbook of Electroencephalography and Clinical Neurophysiology (Vol. 1). Amsterdam, Elsevier.

Gevins, A.S., Zeitlin, G.M., Yingling, C., Doyle, J., Dedon, M., Henderson, J., Schaffer, R., Roumasset, J. & Yeager, C. (1979a) EEG patterns during "cognitive" tasks. Part 1: Methodology and analysis of complex behaviors. EEG Clin. Neurophysiol., 47, 693-703.

Gevins, A., Zeitlin, G., Doyle, J., Schaffer, R. & Callaway, E. (1979b) EEG patterns during "cognitive" tasks. Part 2: Analysis of controlled tasks. EEG Clin. Neurophysiol., 47, 704-710.

Gevins, A.S., Zeitlin, G.M., Doyle, J.C., Schaffer, R.E., Yingling, C.D., Yeager, C.L. & Callaway, E. (1979c) EEG correlates of higher cortical functions. Science, 203, 665-668.

Gevins, A., Doyle, J.C., Schaffer, R.E., Callaway, E. & Yeager, C. (1980) Lateralized cognitive processes and the electroencephalogram. Science, 207, 1005-1008.

Gevins, A., Doyle, J., Cutillo, B., Schaffer, R., Tannehill, R., Ghannam, J., Gilcrease, V. & Yeager, C. (1981) Electrical potentials in human brain during cognition: New method reveals dynamic patterns of correlation of human brain electrical potentials during cognition. Science, 213, 918-922.

Gevins, A.S., Schaffer, R.E., Doyle, J.C., Cutillo, B.A., Tannehill, R.S. & Bressler, S.L. (1983) Shadows of thought: Rapidly changing, asymmetric brain-potential patterns of a brief visuomotor task. Science, 220, 97-99.

Gevins, A.S., Bressler, S.L., Cutillo, B.A., Doyle, J.C. Morgan, N.H. & Zeitlin, G.M. (1984a) Neurocognitive pattern analysis of an auditory and visual numeric motor control task. Part 1: development of methods. Final Report A.F.O.S.R. Contract F49620-82-K-0006, October.

Gevins, A.S., Bressler, S.L., Cuttillo, B.A., Doyle, J.C., Morgan, N.H. & Zeitlin, G.M. (1984b) Neurocognitive pattern analysis. Annual Report ONR Contract N00014-82-C-0022, November.

Gevins, A.S., Doyle, J.C., Cutillo, B.A., Schaffer, R.E., Tannehill, R.S., Bressler, S.L. & Zeitlin, G. (1985) Neurocognitive pattern analysis of a visuomotor task: Low-frequency evoked correlations. Psychophysiology, 22, 32-43.

Hjorth, B. (1975) An on-line transformation of EEG scalp potentials into orthogonal source derivations. EEG Clin. Neurophysiol., 39, 526-530.

Hjorth, B. (1980) Source derivation simplifies topographical EEG interpretation. Amer. J. EEG Technol., 20, 121-132.

Hjorth, B. (1982) An adaptive EEG derivation technique. EEG Clin. Neurophysiol., 54, 654-661.

Hosek, R.S. (1970) An experimental and theoretical analysis of effects of volume conduction in a nonhomogeneous medium on scalp and cortical potentials generated in the brain. Doctoral dissertation, Marquette University.

Janze, C.P. & Kaizer, J.M. (1983) Time-frequency distributions of loudspeakers: the application of the wigner distribution. J. Audio Engr. Soc., 31(4), 198-223.

Jex, H.R. (1978) Defining and measuring perceptual-motor workload in manual control tasks. Systems Technology Inc. Tech. Report 1104-1.

Kavanagh, R. (1972) Localization of sources of human evoked responses. Doctoral dissertation, California Institute of Technology, Pasadena.

Kavanagh, R. N., Darcey, T. M., Lehmann, D. & Fender, D. (1978) Evaluation of methods for three-dimensional localization of electrical sources in the human brain. IEEE Trans. Biomed. Engr., BME-25, 421-429.

McGillem, C. & Aunon, J. (In press) Analysis of event-related potentials. In A. Gevins & A. Remond (Eds.), Handbook of Electroencephalography and Clinical Neurophysiology: Methods of Analysis of Brain Electrical and Magnetic Signals (Vol. 1). Amsterdam, Elsevier.

McGillem, C., Aunon, J. & Childers, D. (1981) Signal processing in evoked potential research: Applications of filtering and pattern recognition. CRC Crit. Rev. Bioengr., 6(3), 225-265.

McGillem, C.D., Aunon, J.I. & Pomalaza, C.A. (1985) Improved waveform estimation procedures for event-related potentials. IEEE Trans. Biomed. Engr., BME-32(6), 371-379.

Morgan, N.H. & Gevins, A.S. (In prep.) Semi-automated editing of EEG.

Nunez, P.L. (1981) Electric fields in the brain: The neurophysics of EEG. New York, Oxford University Press.

Newell, K. (1978) Some issues on action plans. In G. Stelmach (Ed.), Information Processing in Motor Control and Learning. New York, Academic Press, 41-54.

Okada, Y.C. (1983) Inferences concerning anatomy and physiology of the human brain based on its magnetic field. Il Nuovo Cimento, 2, 373-409.

Plonsey, R. (1969) Bioelectric Phenomena. McGraw Hill, New York.

Rosenbaum, D., Saltzman, E. & Kingman, A. (1984) Choosing between movement sequences. In S. Kornblum & J. Requin (Eds.), Preparatory States and Processes. Englewood Cliffs, NJ, Erlbaum, 119-136.

Sternberg, S., Monsell, S., Knoll, R. & Wright, C. (1978) The timing of rapid movement sequences. In G. Stelmach (Ed.), Information Processing in Motor Control and Learning. New York, Academic Press, 117-152.

Thickbroom, G.W., Mastaglia, F.L., Carroll, W.M. & Davies, H.D. (1984) Source derivation: application to topographic mapping of visual evoked potentials. EEG Clin. Neurophysiol., 59, 279-285.

Weinberg, H., Stroink, G. & Katila, T. (Eds.) (1985) Biomagnetism: Applications and Theory. New York, Permagon Press.

Williamson, S.J. & Kaufman, L. (1981a) Biomagnetism. Journal of Magnetism and Magnetic Materials, 22(2), 129-202.

Williamson, S.J. & Kaufman, L. (1981b) Magnetic fields of the cerebral cortex. In S.N. Erne, H.D. Hahlbohm & H. Lubbig (Eds.), Biomagnetism. New York, Walter de Gruyter, 353-402.

Williamson, S.J. & Kaufman, L. (In press) Analysis of neuromagnetic signals. In A. Gevins & A. Remond (Eds.), Handbook of Electroencephalography and Clinical Neurophysiology: Methods of Analysis of Brain Electrical and Magnetic Signals (Vol. 1). Amsterdam, Elsevier.

Williamson, S.J., Romani, G.L., Kaufman, L. & Modena, I (Eds.) (1983) Biomagnetism: An Interdisciplinary Approach. New York, Plenum.

END

DTIC

8-86